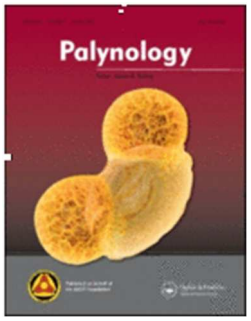

The cyst-theca relation of Trinovantedinium pallidifulvum, with erection of Protoperidinium lousianensis sp. nov. and their phylogenetic position within the Conica group

Journal:	*Palynology*
Manuscript ID	TPAL-2015-0077.R1
Manuscript Type:	Original Article
Date Submitted by the Author:	n/a
Complete List of Authors:	Mertens, Kenneth; Ghent University, Palaeontology; Ifremer, LER BO Gu, Haifeng; Third Institute of Oceanography, SOA Takano, Yoshihito; Institute for East China Sea Research (ECSER) Price, Andrea; McGill University, Geography Pospelova, Vera ; University of Victoria, School of Earth and Ocean Sciences Bogus, Kara; International Ocean Discovery Program, Texas A&M University Versteegh, Gerard; MARUM – Center for Marine Environmental Sciences; Alfred-Wegener-Institut (AWI), Helmholtz Zentrum für Polar und Meeresforschung Marret-Davies, Fabienne ; School of Environmental Sciences, University of Liverpool Turner, R. ; Louisiana State University, Department of Oceanography and Coastal Sciences, Rabalais, Nancy; Louisiana Universities Marine Consortium Matsuoka, Kazumi; Institute for East China Sea Research (ECSER)
Keywords:	Gulf of Mexico, Saanich Inlet, microFTIR, Selenopemphix undulata, Wadden Sea, lake Saroma

The cyst-theca relation of *Trinovantedinium pallidifulvum*, with erection of *Protoperidinium lousianensis* sp. nov. and their phylogenetic position within the *Conica* group

Kenneth Neil Mertens[1*†], Haifeng Gu[2], Yoshihito Takano[3], Andrea M. Price[4], Vera Pospelova[5], Kara Bogus[6], Gerard J. M. Versteegh[7‡], Fabienne Marret[8], R. Eugene Turner[9], Nancy N. Rabalais[10], Kazumi Matsuoka[3]

[1]Research Unit for Palaeontology, Ghent University, Krijgslaan 281 s8, 9000 Ghent, Belgium
[2]Third Institute of Oceanography, SOA, Xiamen 361005, China, guhaifeng@tio.org.cn
[3]Institute for East China Sea Research (ECSER), 1551-7, Taira-machi, Nagasaki, 851-2213, Japan, takadino@gmail.com, kazu-mtk@nagasaki-u.ac.jp
[4]Department of Geography, McGill University, Burnside Hall, 805 Sherbrooke Street West, Montreal, QC, Canada H3A OB9, andrea.price@mail.mcgill.ca
[5]School of Earth and Ocean Sciences, University of Victoria, OEASB A405, P.O. Box 1700 STN CSC, Victoria, British Columbia, V8W 2Y2, Canada, vpospe@uvic.ca
[6]International Ocean Discovery Program, Texas A&M University, 1000 Discovery Drive, College Station, TX, USA 77845, bogus@iodp.tamu.edu
[7]MARUM – Center for Marine Environmental Sciences, Leobener Strasse, 28359 Bremen, Germany, versteegh@uni-bremen.de
[8]School of Environmental Sciences, University of Liverpool, Liverpool, L69 7ZT, UK f.marret@liv.ac.uk
[9]Department of Oceanography and Coastal Sciences, Louisiana State University, Baton Rouge, Louisiana 70803 USA, euturne@lsu.edu
[10]Louisiana Universities Marine Consortium, Chauvin, Louisiana 70344 USA, nrabalais@lumcon.edu

We establish the cyst-theca relationship of the cyst species *Trinovantedinium pallidifulvum* Matsuoka 1987 based on germination experiments of specimens isolated from the Gulf of Mexico. We show that the motile stage is a new species, designated as *Protoperidinium louisianensis*. We also determine its phylogenetic position based on single-cell PCR of a single cell germinated from the Gulf of Mexico cysts. To further refine the phylogeny, we determined the LSU sequence through single-cell PCR of the cyst *Selenopemphix undulata* isolated from Brentwood Bay (Saanich Inlet, BC, Canada). The phylogeny shows that *P. louisianensis* is closest to *P. shanghaiense,* the motile stage of *T. applanatum,* and ~~leave the possibility~~is consistent with ~~that the~~the monophyly of the genus *Trinovantedinium* ~~is monophyletic~~. *Selenopemphix undulata* belongs to a different clade than *Selenopemphix quanta* (alleged cyst of *P. conicum*), suggesting that the genus *Selenopemphix* is polyphyletic. *Trinovantedinium pallidifulvum* is widely distributed with occurrences in the Gulf of Mexico, the North Atlantic, the NE Pacific and SE Asia. In addition, we illustrate the two other extant species, *Trinovantedinium applanatum* and *Trinovantedinium variabile* and two morphotypes of *Trinovantedinium*. Geochemical analyses of the cyst wall of *T. pallidifulvum* indicate the presence of amide groups in

* Now at: Ifremer, LER BO, Station de Biologie Marine, Place de la Croix, BP40537, F-29185 Concarneau Cedex, France, kenneth.mertens@ifremer.fr
† Corresponding author. Email: kenneth.mertens@ifremer.fr
‡ Now at: Alfred-Wegener-Institut (AWI). Helmholtz Zentrum für Polar und Meeresforschung, Am Handelshafen 12, D-27570, Bremerhaven, Germany, gerard.versteegh@awi.de

agreement with other heterotrophic dinoflagellate species, although the cyst wall cyst of *T. pallidifulvum* also includes some unique features.

Keywords: microFTIR; *Selenopemphix undulata*; Wadden Sea; lake Saroma; Saanich Inlet; Gulf of Mexico

1. Introduction

The heterotrophic thecate dinoflagellate genus *Protoperidinium* Bergh is characterized by possessing three cingular plates and an additional transitional plate (Balech 1974). This large genus currently encompasses approximately 280 species (Gómez 2012). The identification of the thecate stage of *Protoperidinium* species is based on the body size, outline, presence and position of apical and/or antapical horns/spines, cingulum displacement and particularly the plate pattern (e.g., Hoppenrath et al. 2009). In regard to the thecal plate arrangement, Balech (1974) used the number of anterior intercalary plates and precingular plates to subdivide *Protoperidinium* into three subgenera: the subgenus *Protoperidinium*, which has seven precingular plates and three anterior intercalary plates; the subgenus *Minusculum*, which has six precingular plates and three anterior intercalary plates; and the subgenus *Archaeperidinium*, which has seven precingular plates and two anterior intercalary plates. Later, the subgenus *Testeria* was erected by Faust (2006) to accommodate species with seven precingular plates, one anterior intercalary plate and no apical pore complex. However, the results from molecular phylogeny questioned the validity of the subgenus *Minusculum* because it was nested within the subgenus *Protoperidinium* (Yamaguchi et al. 2007; Ribeiro et al. 2010), and showed the polyphyly of the subgenus *Archaeperidinium*, as originally described by Jörgensen (1912) (Ribeiro et al. 2010). *Archaeperidinium* was, therefore, emended as a genus and characterized by the flat sulcus, sulcal flagellar fin covering the sulcal area and circular cingulum without displacement (Yamaguchi et al. 2011).

The subgenus *Protoperidinium* can be subdivided into several sections based on the shape of the first apical (1′) plate (ortho, meta or para) and the shape of the second anterior intercalary (2a) plate (quadra, penta or hexa) (e.g., Gribble and Anderson 2006). Molecular phylogenies suggested that most of these sections are monophyletic and nested within the *Protoperidinium* sensu stricto clade (Mertens et al. 2013; Gu et al. 2015). There are only two exceptions: the section *Conica* is polyphyletic and positioned within the *Protoperidinium* sensu stricto clade (Yamaguchi et al. 2006; Gu et al. 2015), and the section *Oceanica* is monophyletic but positioned outside of the *Protoperidinium* sensu stricto clade (Sarai et al. 2013).

Several *Protoperidinium* species have been associated with~~to~~ a particular cyst, and the morphology of these cysts can be taxonomically informative, especially the shape of ~~the opening in the cyst wall, termed~~ the archeopyle (Harland 1982). Thecate stages belonging to *Protoperidinium* and *Archaeperidinium* with a transitional plate have cysts generally ~~have~~with a saphopylic or theropylic 2a archeopyle ~~of their respective cyst~~ (Harland 1982; Ribeiro et al. 2010; Mertens et al. 2012a) whereas, *Protoperidinium* species without a transitional plate have cysts with a compound archeopyle involving 2′–4′ (Lewis & Dodge 1987; Kawami & Matsuoka 2009; Kawami et al. 2009; Mertens et al. 2013; Liu et al. 2014). Cyst morphology can be diverse and is used to classify cysts into various cyst-defined genera such as *Brigantedinium* Reid, *Votadinium* Reid and *Selenopemphix* Benedek (Fensome et al. 1993). However, differences between the cyst-~~based~~ defined nomenclature and the motile-~~based~~ defined nomenclature have not yet been fully reconciled.

Trinovantedinium Reid is a cyst-~~based~~ defined genus erected by Reid (1977) to describe peridiniacean cysts with an intercalary archeopyle because, at that time, the existence of such an archeopyle in the genus *Lejeunecysta* Artzner & Dörhöfer 1978 was in doubt. This initial diagnosis included species with or without processes on the cyst. The genus was subsequently emended by Harland (1977), Bujak (1984) and de Verteuil & Norris (1992). The latter restricted the diagnosis of *Trinovantedinium* to only include biphragmal cysts with short, penitabular and intratabular, but never sutural, hollow to solid processes. There are currently 11 species within this genus (Table 1). The type species was described by Reid (1977) and is the large transparent *Trinovantedinium capitatum* from ~~recent~~ modern Rosslare Point sediment (Ireland). Later, this was considered a junior synonym of *Lejeunia applanata*, described by Bradford (1977) from recent sediments off the east coast of the Musandam Peninsula (Oman), which was renamed later as *Trinovantedinium applanatum* (for details see de Verteuil & Norris 1992, p. 408). This is the first of only three species from this genus that are considered extant; the other eight species are extinct (Table 1). *Trinovantedinium pallidifulvum* is the second extant species, first described by Matsuoka (1987) from Holocene surface sediments in Akkeshi Bay (Hokkaido, Japan). The third is *Trinovantedinium variabile,* described by Bujak (1984) from the early Pliocene of the Bering Sea, and was recorded as extant by Radi & de Vernal (2004), Pospelova et al. (2008), Krepakevich & Pospelova (2010), Price & Pospelova (2011) and Bringué et al. (2013).

For only one of these extant species is the cyst-theca relationship and molecular phylogenetic position known. The cyst-theca relationship for the type species *Trinovantedinium applanatum* was first established by Wall & Dale (1968); however, it was mistakenly related to *Protoperidinium pentagonum* (Gran) Balech. This error was propagated in subsequent studies (Matsuoka 1982; Lewis et al. 1984; Baldwin 1987). It was Inoue, H. in Fukuyo et al. (1990, p. 154–155) who first remarked that the cingulum of the *T. applanatum* thecate stage has no displacement, in contrast with *P. pentagonum*. Gu et al. (2015) re-established the cyst-theca relationship for *T. applanatum* from the East China Sea, and they erected the species *Protoperidinium shanghaiense* to describe the motile stage. The hexa-ortho configuration placed this species in the *Conica* group and its LSU rDNA sequence was closest to *P. divaricatum, P. leonis* and *P. conicum*. This cyst-theca relationship was most recently confirmed by Li et al. (2015).

In this study, we establish the cyst-theca relationship for the second extant species of the genus *Trinovantedinium, T. pallidifulvum,* through incubation of surface sediments from the Gulf of Mexico, Dee Estuary (United Kingdom), and Wadden Sea (Germany). We erect a new species, *Protoperidinium louisianensis,* to describe the motile stage of *Trinovantedinium pallidifulvum*. We obtained LSU rDNA sequences through single-cell PCR that show the motile stage is closest to *Protoperidinium shanghaiense.* In addition, we document the distribution of *Trinovantedinium pallidifulvum* and the geochemical composition of its cyst wall. We also illustrate the two other extant species, *Trinovantedinium applanatum* and *Trinovantedinium variabile.* Finally, to further constrain the phylogeny, we also resolve the phylogenetic position of *Selenopemphix undulata* from Brentwood Bay (B.C., Canada).

2. Material and methods

2.1. Germination experiments

We collected cysts of *Trinovantedinium pallidifulvum* for incubation studies from surface sediment samples at three locations: (1) northern Gulf of Mexico, (2) Dee Estuary (UK), and (3) the Wadden Sea in northern Germany (Figure 1 and Table 2). All samples were stored in plastic

bags and refrigerated at 4 °C. In situ sea-surface salinities (SSSs) and sea-surface temperatures (SSTs) were measured when collecting the samples (Table 2).

Approximately 0.5–1.0 cm^3 of wet sediment was immersed in filtered seawater after which it was ultrasonicated in a bath (60 s) and rinsed through a 20 µm nylon mesh using filtered seawater. The cyst fraction was separated from this residue using heavy liquid sodium polytungstate (density = 1.3 g cm^{-1}) (Bolch 1997). Single cysts were then transferred to Nunclon 0.5 ml microwells subjected to an irradiance of 100 µmol photons m^{-2} s^{-1} and 24 h light, and filled with L1 medium. The wells were kept at room temperature. Cysts were regularly checked for germination, and observations were performed under an Leitz DM inverted light microscope. Encysted and excysted cysts as well as motile cells were photographed and measured using an Leica DM 5000B light microscope equipped with a Leica DFC 490 camera with 100x oil immersion objectives. For each motile cell, the length, width, depth, distance between the tips of the antapical horns, and width of the cingulum were measured, ~~as~~ where possible. For each cyst, the same parameters were measured; additionally, the length of three randomly chosen spines per cyst were measured. All measurements in the species descriptions cite, in order: the minimum, average (in parentheses) and maximum values (in µm). The standard deviation (SD) is also provided where appropriate.Incubation experiments were done by KNM and took place at GEOTOP (Gulf of Mexico and Dee Estuary samples) and Univ. of Bremen (Wadden Sea samples). All measurements were done by KNM.

We also attempted to germinate *Selenopemphix undulata* from Saanich Inlet (Canada), but none of the isolated cysts germinated.

2.2. Study of cysts from surface sediments

To determine the distribution of *Trinovantedinium pallidifulvum*, permanent slides of surface samples were examined which included locations from the the northeastern and northwestern Pacific and the northern Gulf of Mexico (Figure 1 and Table 2). Routine palynological techniques were used for processing (Pospelova et al. 2004; Matsuoka et al. 2003; Mertens et al. 2012b). The samples were oven-dried at 40 °C and then treated with room-temperature 10% hydrochloric acid (HCl) to remove calcium carbonate. The material was rinsed twice with distilled water, sieved at 120 µm to eliminate the coarse fraction, and retained on a 15 µm nylon mesh. To dissolve siliceous particles, samples were treated with 48–50% room-temperature hydrofluoric acid (HF) for at least two days, and then treated for 10 min with room-temperature HCl (10%) to remove fluorosilicates. The residue was rinsed twice with distilled water, ultrasonicated for 30 s and finally collected on a 15 µm mesh. Residue aliquots were mounted in glycerine jelly. All measurements and light photomicrographs were as described in Section 2.1. In addition, in order to illustrate *Trinovantedinium applanatum* and *Trinovantedinium variabile,* we re-examined permanent slides from palynologically prepared samples from several localities.

2.3. Single-cell PCR amplification and sequencing of the motile stage of **Trinovantedinium pallidifulvum**

Surface sediment samples containing *Trinovantedinium pallidifulvum* were used from the Gulf of Mexico (Figure 1 and Table 2). Cysts were isolated from the sediment using the heavy liquid separation described in Section 2.1. Motile cells identified through light microscopy were rinsed several times in sterilized distilled water, broken by compressing the cell between the slide and cover slip, and then transferred into a PCR tube. The single cell was used as the template to amplify about 1200 bp of the nuclear-encoded LSU rDNA, using the primers D1R (Scholin et al.

1994) and 28-1483R (Daugbjerg et al. 2000). A 50 µl PCR cocktail containing 0.2 µM primers, PCR buffer, 50 µM dNTP mixture, 1U of Ex Taq DNA polymerase (Takara, Dalian, China) was subjected to 35 cycles using a Mastercycler PCR (Eppendorf, Hamburg, Germany). The PCR protocol was: initial denaturation for 3.5 min at 94 ºC, followed by 35 cycles of 50 s denaturation at 94 ºC, 50 s annealing at 45 ºC, and 80 s extension at 72 ºC, plus a final extension of 10 min at 72 ºC. The amplified products were run on a 1% agarose gel. Positive bands were excised and purified using a DNA extraction kit (Sangon, Shanghai, China) and sequenced in both directions using the ABI Big-Dye dye-terminator technique (Applied Biosystems, Foster City, California, USA), according to the manufacturer recommendations. This DNA work was performed by HG in Third Oceanographic Centre, Xiamen, China.

2.4. Single-cell PCR amplification and sequencing of cysts of Selenopemphix undulata

We obtained surface sediment samples containing *Selenopemphix undulata* from Brentwood Bay (B.C., Canada) (48,58°N,-123.47°E, 6 m water depth) using a petite ponar grab on October 1, 2011. Cysts were isolated from the sediment using heavy liquid separation as described in Section 2.1. The cysts were then rinsed several times in sterilized distilled water, broken by compressing the cell between the slide and cover slip, and then transferred into a PCR tube. The single cell was used as the template to amplify about 1200 bp of the nuclear-encoded LSU rDNA, using the primers D1R (Scholin et al. 1994) and 28-1483R (Daugbjerg *et al.* 2000). A 50 µl PCR cocktail containing 0.2 µM primers, PCR buffer, 50 µM dNTP mixture, 1U of Ex Taq DNA polymerase (Takara, Dalian, China) was subjected to 35 cycles using a Mastercycler PCR (Eppendorf, Hamburg, Germany). The PCR protocol was an initial denaturation for 3.5 min at 94 ºC, followed by 35 cycles of 50 s denaturation at 94 ºC, 50 s annealing at 45 ºC, and 80 s extension at 72 ºC, plus a final extension of 10 min at 72 ºC. The amplified products were run on a 1% agarose gel. Positive bands were excised and purified using a DNA extraction kit (Sangon, Shanghai, China) and sequenced in both directions using the ABI Big-Dye dye-terminator technique (Applied Biosystems, Foster City, California, USA), according to the manufacturer's recommendations. This DNA work was performed by YT at the University of Nagasaki, Japan.

2.5. Sequence alignments and phylogenetic analyses

Newly obtained sequences were first aligned with those of related species available in GenBank using 'BioEdit' v7.0.0 (Hall 1999), and subsequently using Mafft (Katoh et al. 2005) (http://mafft.cbrc.jp/alignment/server/). *Akashiwo sanguinea* (Hirasaka) G. Hansen & Moestrup was selected as the outgroup. A Bayesian reconstruction of the data matrix was performed with MrBayes 3.0b4 (Ronquist & Huelsenbeck 2003) using a general time reversible model (GTR +I+G) chosen byJmodelTest (Posada 2008). Four Markov chain Monte Carlo (MCMC) chains ran for two million generations, sampling every 1,000 generations with a burnin of 10%. A majority rule consensus tree was created in order to examine the posterior probabilities of each clade. Maximum likelihood-based analyses were conducted with RaxML v7.2.6 (Stamatakis 2006) on the T-REX web server (Boc et al. 2012) using the above model. Bootstrap values were determined with 1,000 replicates.

2.6. Geochemical analysis of cyst wall chemistry

After germination, an empty cyst originally derived from surface sediment of the Wadden Sea (Germany) (Figure 1) was removed from a microwell using a micropipette into a droplet of water contained on a glass slide with a concave depression. The water was allowed to evaporate and

then a droplet of ethanol was added. The cyst was allowed to soak in the ethanol for 30 min after which a droplet of MilliQ water was added. The cyst was then isolated and the procedure repeated twice. These steps were to ensure that any polar or apolar compounds adhered to the cyst wall were removed. The cyst was then visually examined under the light microscope and placed on an Au-coated mirror and analysed with micro-Fourier transform infrared spectroscopy using a Bruker FT-IR microscope (Hyperion 3000) with a 15x objective. The spectrum was acquired in reflective mode with 50 scans over 4000-600 cm^{-1} and is shown after background subtraction. Peak assignments were based on Colthup (1990) and relevant published literature (e.g., Bogus et al. 2012; 2014; Cárdenas et al. 2004; Versteegh et al. 2012). This geochemical work was done by KB, KNM and GJMV at the Univ. of Bremen, Germany.

3. Results

3.1. Results of germination experiments

Undescribed motile cells, here assigned to *Protoperidinium louisianensis* n. sp., emerged from *Trinovantedinium pallidifulvum* cysts isolated from surface sediments of the Gulf of Mexico (five specimens identified) (Figure 1 and Table 1). These motile cells germinated from the cysts a~~A~~fter one or two days of incubation~~, motile cells germinated from the cysts~~. The~~se~~ cells died a few days after germination and never divided. Two out of four specimens of *Trinovantedinium pallidifulvum* from the Wadden Sea (Germany) germinated, but the cells did not fully develop thecal plates. A single specimen from the Dee Estuary (UK) germinated, but the motile stage could not be fully observed.

3.2. Systematic pal~~a~~eontology

Division DINOFLAGELLATA (Bütschli 1885) ~~emend.~~ Fensome et al. 1993, emend. Adl et al. 2005

Class DINOPHYCEAE Pascher 1914

Subclass PERIDINIPHYCIDAE Fensome et al. 1993

Order PERIDINIALES Haeckel 1894

Family PROTOPERIDINIACEAE Balech 1988 nom. cons.

Subfamily PROTOPERIDINIOIDEAE (Autonym)

Genus *Protoperidinium* Bergh 1881

Protoperidinium louisianensis Mertens, Gu, Price et Matsuoka n. sp.

Plate 1, figures 1–15, Plate 2, figures 1-15

Holotype. Plate 1, figures 1–9.

Type locality. Northern Gulf of Mexico, station A7 (28.94°N, 89.75°W), offshore Louisiana.

Diagnosis. A species of intermediate size of the genus *Protoperidinium* with the tabulation formula Po, X, 4′, 3a, 7″, 3c+t, ?s, 5‴, 2⁗. The motile cell is pentagonal in outline and dorsoventrally flattened, with a short apical horn and two antapical horns, each bearing a short spine. The epitheca is longer than the hypotheca, and bears convex sides. Plate 1′ is ortho-type, 1a and 3a are penta-type, and 2a is hexa-type and stenodeltaform linteloid. Plates are thin with polygonal reticulations. The cyst is pentagonal and light brown in color, with a thickened apical horn and two thickened antapical horns. The cyst surface is smooth, bearing numerous peritabular, short, solid, erect, and non-branching processes with acuminate tips. Sometimes the dorsal side of the hypotheca is striated. The archeopyle is stenodeltaform linteloid, angular and saphopylic.

Derivation of name. The specific epithet refers to the type locality, which lies~~is~~ offshore the state of Louisiana (USA).

Gene sequence. The LSU rDNA gene sequence of the cyst—GenBank Accession No. KU519754~~XXXXXX~~ (LSU).

Description. *Description of motile cell of* Protoperidinium louisianensis *(Plate 1, figures 1–9, Plate 2, figures 1-9).* The excysted motile cells (five observed and not preserved) were pentagonal in outline, dorsoventrally flattened and carried an apical horn and two antapical horns of equal length, each bearing a short spine (Plate 1, figure 1-2, Plate 2, figure 1). The epitheca had convex sides and was longer than the hypotheca. The cell contents were greenish, except for a red body. The thin thecal plates carried polygonal reticulations (Plate 1, figure 2,7).

The plate arrangement on the epitheca was bilaterally symmetrical. The oval apical pore plate (Po) was surrounded by a low apical collar formed by the raised edges of the apical plates (Plate 2, figure 4). The canal plate (X) was elongate and trapezoidal (Plate 2, figure 4). The first apical plate (1′) was wide and rhombic (ortho-type) and the sides of plate 1′ contacting plates 2′ and 4′ are longer than those contacting plates 1″ and 7″ (Plate 1, figure 2). Plates 2′ and 4′ were elongated and subpentagonal, whereas 3′ was short and subpentagonal (Plate 1, figure 4). The first and third anterior intercalary plates (1a) were pentagonal and equal in size (Plate 1, figures 3,6). The second anterior intercalary plate (2a) was hexagonal, stenodeltaform linteloid and more elongated and had two small sides touching plates 3″ and 5″ (Plate 1, figure 4). The precingular series consisted of seven plates. Plate 1″, 4″ and 7″ were quadrangular (Plate 1, figures 2,4), and 2″, 3″, 5″ and 6″ pentagonal (Plate 1, figures 3,5,6). The cingulum was slightly left-handed (descending), lined with narrow lists and comprising three cingular plates plus a transitional plate. The transitional plate (t) was small. Plate 1c reached the end of plate 1″ and 2‴ (Plate 1, figure 3). Plate 2c was the longest of the series and reached a short way beyond the 6″/7″ boundary and the 4‴/5‴ boundary (Plate 1, figure 7). Plate 3c was similar in size to Plate 1c.

We were unable to dissect and observe all the sulcal plates.

The plate arrangement of the hypotheca was also symmetrical, featuring five postcingular plates. Plate 5‴ was longer than plate 1‴. Plates 1‴, 3‴, and 5‴ were pentagonal, and 2‴ and 4‴ were quadrangular (Plate 1, figures 7-9). The antapical series comprised two plates, 1⁗ and 2⁗, which formed the antapical horns (Plate 1, figure 7).

The plate formula is thus Po, X, 4′, 3a, 7″, 3c+t, ?s, 5‴, 2⁗, and the complete tabulation (except for the sulcal plates) is illustrated in Figure 2.

Description of cyst of Protoperidinium louisianensis *(Plate 1, figures 10–15, Plate 2, figures 10-15).* Cysts were similar in shape to the motile stage, but light brown in color, bearing numerous small solid spines. The cysts were peridinioid (pentagonal) with a thickened apical horn and two thickened antapical horns of equal length. Living cysts contained abundant greenish granules. The epicyst had convex sides and was always longer than the hypocyst. The central body wall was thin (>0.3 µm) and biphragmal with closely appressed layers that separate along the apical horn and antapical horns, with a smooth surface (Plate 1, figure 11). Sometimes striations were present on the dorsal side of the hypocyst (Plate 2, figure 15). The processes were short, solid, erect, and non-branching with acuminate tips (Plate 1, figure 11). The process distribution was largely ~~peritabular~~ penitabular (Plate 1, figure 13, Plate 2, figure 11). The process length was fairly constant for individual specimens, except around the apical horn and antapical horns where they became longer (Plate 2, figure 10). The ~~para~~cingulum was excavated with lists ornamented with rows of equidistant processes, and slight left-handed displacement (Plate 2, figure 11). The ~~para~~sulcus was free of processes and indented (Plate 1, figure 14), two flagellar scars were

Formatted: Font: Times New Roman, 12 pt

always visible (Plate 2, figure 12). The archeopyle was angular and saphopylic, involving release of plate 2a, steno-deltaform linteloid. The description is based on cysts used in the incubation experiments and those recovered from sediment and prepared using palynological methods. Cysts without cell content in the palynologically treated samples did not retain their shape well - they did not seem to be very robust as they were always quite folded and flattened.

Dimensions. Incubated motile cells: length, 52.3 (58.8) 65.1 µm (SD = 6.0, n=4); width, 44.0 (53.6) 58.8 µm (SD = 7.4, n=4); depth, 34.8 (38.4) 41.9 µm (SD = 5.0, n=2); distance between the tips of the antapical horns, 12.8 (16.3) 20.3 µm (SD = 3.7, n=4); width of cingulum, 3.9 (4.1) 4.4 µm (SD = 0.2, n=4).

Cysts germinated to give identifiable thecae: length, 43.0 (58.5) 68.4 µm (SD = 8.2, n=10); width, 46.3 (56.5) 63.9 µm (SD = 5.0, n=10); depth, 30.4 (40.6) 48.4 µm (SD = 7.2, n=7); distance between the tips of the antapical horns, 16.0 (23.9) 27.7 µm (SD = 3.6, n=10); width of cingulum, 4.5 (6.0) 7.2 µm (SD = 0.8, n=10); average length of three spines per cyst, 1.1 (1.8) 2.7 µm (SD = 0.4, n=30).

Cysts palynologically prepared from surface sediments of different locations: length, 49.9 (56.6) 62.8 µm (SD = 5.7, n=5); width, 49.8 (56.3) 63.3 µm (SD = 5.0, n=5); depth, none measured; distance between the tips of the antapical horns, 20.6 (21.3) 22.5 µm (SD = 0.8, n=5); width of cingulum, 4.8 (5.6) 6.5 µm (SD = 0.7, n=4); average length of three spines per cyst, 1.4 (1.9) 2.8 µm (SD = 0.4, n=15).

Comments. The geological preservability of the cysts was demonstrated by their ability to withstand palynological treatment and presence in sediments at least as old as Holocene (Matsuoka et al. 1999) to mid-Miocene (our interpretation of the "undefined protoperidiniacean species" depicted in de Verteuil & Norris (1992), plate 2, figs. 9–12). Specimens from the German Wadden Sea show an identical morphology (Plate 3, figures 1–12) and the cysts correspond to the cyst-~~based~~ defined species~~taxon~~ *Trinovantedinium pallidifulvum* Matsuoka, here reillustrated by its holotype (Plate 3, figures 13–16).

Genus *Trinovantedinium* Reid 1977, emend. de Verteuil & Norris 1992

Tinovantedinium applanatum (Bradford 1977) Bujak & Davies 1983

Plate 4, figures 1–13, Plate 5, figures 1-10

Synonyms. *Trinovantedinium capitatum* Reid 1977, Plate 1, figures 6–8.

Comments. The illustrated specimens conform to the original description of Bradford (1977). We also illustrate two extreme morphotypes of this species. Type A (Plate 5, figures 1–7) was found in warmer water regions (Omura Bay, Japan; Bay of Bengal; Red Sea) and shows a more elongate, transparant body shape with straight sides and more elongated horns, separated by a deep depression. Type B (Plate 5, figures 8–10) was found in cold water (offshore Greenland) and shows a more rounded, transparent body shape with reduced horns and a very shallow depression between the antapical horns. *Trinovantedinium applanatum* differs form *Trinovantedinium pallidifulvum* in its transparency, often larger and more elongate body and longer processes.

Trinovantedinium variabile (Bujak 1984) de Verteuil & Norris 1992

Plate 6, figures 1–11

Comments. The illustrated specimens conform to the original description of Bujak (1984). The holotype is redescribed and reillustrated by Head (1994, p. 226, pl. 11, figs. 4,5,7,8).

Formatted: French (France)

Genus *Selenopemphix* Benedek 1972, emend. Head 1993

Selenopemphix undulata Verleye, Pospelova, Mertens et Louwye 2011, Plate 1, figure 8

Plate 6, figures 12–14

Comments. One cyst corresponding to *Selenopemphix undulata* as described by Verleye et al. (2011, particularly the specimen displayed in Plate 1, figure 8) was isolated for single-cyst PCR (Plate 6, figures 12–14). The cyst was collected from surface sediment of Brentwood Bay (B.C., Canada). The cyst was large and polar compressed, with a cingulum with ~~undulating~~ margins showing very small undulations. The epicyst was conical and striated, the hypocyst was also striated and bore two fused antapical horns that were wider than the apical horn. The archeopyle could not be observed on encysted specimens. The single cyst had a length of 44.5 µm (apex to antapex), width of 74.6 µm, and depth of 70.8 µm.

Gene sequence. The LSU rDNA gene sequence of the cyst—GenBank Accession No. LC114019 (LSU).

3.3. Phylogenetic position of Protoperidinium louisianensis *and* Selenopemphix undulata *as inferred from LSU rDNA sequences*

We obtained 1,143 base pairs from one germinated cell of *Protoperidinium louisianensis* isolated from the Gulf of Mexico (Accession number: KU519754~~XXXXXX~~), and this sequence was used for the phylogenetic analyses (Figure 3). *Protoperidinium louisianensis* was closest to *Protoperidinium shanghaiense*, and formed a clade with several other species belonging to the *Conica* section (*P. divaricatum, P. conicum, P. leonis*). *Selenopemphix undulata* (Accession number: LC114019), was closest to *Protoperidinium biconicum,* which also belongs to the section *Conica* and formed a separate clade with *P. punctulatum* and *P. humile*, both species belonging to the section *Tabulata*. The other members of the Protoperidiniaceae formed several other clades, which were also used by Gu et al. (2015).

Formatted: Font: Times New Roman, 12 pt

3.4. Modern ~~Recent d~~distribution of Trinovantedinium pallidifulvum *and inferred ecology*

Trinovantedinium pallidifulvum was initially described by Matsuoka (1987) from Akkeshi Bay (Hokkaido, Japan) and subsequently predominantly in southeast Asia, ~~such as~~including surface sediments off South Korea (Cho et al. 2003; Shin et al. 2011), Japan (Kojima et al., 1994; Matsuoka et al. 2003), China (Wang et al. 2004), and Malaysia (Furio et al. 2006) (Figure 1)).

In this study we show that this species is much more widely distributed since it is recorded in surface sediments from the northern Gulf of Mexico, Casino Coast (Brazil), the North Atlantic (La Vilaine Bay, Wadden Sea (Germany), Dee Estuary (UK), Kattegat), NW Pacific (Tokyo Bay and Ariake Sound, both in Japan) and the NE Pacific (Vancouver Island, Canada) (Table 2 and Figure 1). We also identify a specimen from the German Bight depicted by Nehring (1997, his figures 23–24, as *Trinovantedinium capitatum*) also as *T. pallidifulvum*. The highest relative abundance of *T. pallidifulvum* ~~cysts~~ was recorded in a surface sample from the Gulf of Mexico where it~~the cysts~~ contributes up to 3.8% of the cyst assemblages (Table 2). *T. pallidifulvum* was found in this study in surface sediment samples corresponding to SSTs of ~11.30–31.45 °C and SSSs with a range of 8.60–33.61 psu (Table 2).

3.5. Trinovantedinium pallidifulvum *cyst wall chemistry*

The spectrum produced by micro-FTIR analysis of the cyst wall (Figure 4) shows: a broad peak centered at 3340 cm^{-1} (OH stretching), weak peaks at 2920 and 2860 cm^{-1} (aliphatic CH stretching), peaks at 1780 and 1700 cm^{-1} (C=O stretching), 1630 cm^{-1} (C=C, C=O stretching

(amide I)), 1585 and 1560 cm^{-1} (CN stretching, NH bending (amide II)), 1440 and 1405 cm^{-1} (CH bending), 1350 cm^{-1} (NO_2, CCH_3 (not indicated in Figure 4)), 1310 cm^{-1} (amide III), 1255 cm^{-1} (NH bending), 1140 and 1030 cm^{-1} (C-O stretching), and 890, 850 and 770 cm^{-1} (CH out of plane).

4. Discussion

4.1. Comparative morphology of the motile stage of P. louisianensis *within the* Conica *group*

The motile stage of *P. louisianensis* can be distinguished from all species from the *Conica* group by the unique combination of excavated antapical horns each bearing a single spine, an epitheca with convex sides being longer than the hypotheca, a slightly left-handed cingulum, a stenodeltaform linteloid 2a and plates with polygonal reticulations. A few species show strong similarities. *P. conicum* also has spines on the antapical horns, but has an epitheca that is as long as the hypotheca, straight sutures from the apex to the cingulum and a more elongated pore (Gu et al. 2015). *P. shanghaiense* has no displacement of the cingulum, an epitheca with straight sides, two relatively closer antapical horns that bear no spines and a 2a that was isodeltaform linteloid (Gu et al. 2015). *P. conicoides* also bears spines on the antapical horns, but is more polar compressed. It also has an epitheca that is as long as the hypotheca, a 1‴ which has a "nose" at the onset of the sulcus, and straight sutures from the apex to the cingulum (Hoppenrath et al. 2009, p. 158). The plates of *P. obtusum* and *P. leonis* are ornamented with longitudinal ribs (Hoppenrath et al. 2009, p. 158–159).

4.2. Comparative morphology of the cyst of P. louisianensis *within the* Conica *group*

The cyst of *P. louisianensis,* which corresponds to the cyst-~~based~~ defined species~~taxon~~ *Trinovantedinium pallidifulvum,* can be easily differentiated from all other species belonging to the genus *Trinovantedinium* (Table 1). The species differs from *Trinovantedinium applanatum* and *Trinovantedinium henrietii* because these are transparant and have an epicyst the same length as the hypocyst (Matsuoka 1987, Louwye et al. 2008). *Trinovantedinium boreale* is also transparant and has processes with platforms (Bujak 1984; see also Head 1994). *Trinovantedinium glorianum* has much more densely distributed and hollow processes and antapical horns that are sharper (Head et al. 1989). *T. variabile, T. harpagonium, T. ferrugnomatum* and *T. sterthense* are more polar compressed with rounded antapical horns and bear longer processes with distal platforms or taeniate or aculeate processes (Bujak 1984, de Verteuil & Norris 1992, Head 1993). *Trinovantedinium papula* and *Trinovantedinium? xylochoporum* are much more rounded and have longer processes (de Verteuil & Norris 1992).

Formatted: Font: Not Italic

4.3. Validity of the ~~genus~~ genera Trinovantedinium *and* Selenopemphix

The molecular phylogeny shows that *P. louisianensis* and *P. shanghaiense* are most closely related, which is thus the case for their respective cysts, *Trinovantedinium pallidifulvum* and *Trinovantedinium applanatum*. This ~~supports~~ is consistent with the monophyly of the genus *Trinovantedinium*. Whether this will be supported by the molecular characterization of the other extant species, *Trinovantedinium variabile,* should be the subject of further study.

The phylogenetic position of *Selenopemphix undulata* is more problematic because it is positioned in another clade than *Protoperidinium conicum,* the motile stage associated with the cyst-based taxon *Selenopemphix quanta* (note that this cyst-theca relationship needs further study, e.g. Matsuoka & Head 2013). This polyphyly suggests that both species belong to two

different genera, and their relatively long genetic distance suggests that they diverged a long time ago. This polyphyly is also supported by significant morphological differences between species of both cyst types, particularly the position of the archeopyle, which is more offset in *Selenopemphix undulata* (Verleye et al. 2009) than *Selenopemhix quanta* (it is considered central or slightly offset, see Head 1993, p. 31-32). It is, therefore, likely that *Selenopemphix quanta* should be transferred back to its initial name, *Multispinula quanta*. However, we suggest that the molecular phylogenetic position of the type species of *Selenopemhix, Selenopemphix nephroides,* the cyst considered to belong to *Protoperidinium subinerme* (Rochon et al. 1999) needs to be established before such a transfer. Either way, this result emphasizes the importance of the archeopyle position in cyst taxonomy, whereas the reniform cyst shape of both species, seems to be polyphyletic.

4.4. Validity of the genus Protoperidinium

Since long there has been a mismatch between paleontological and biological names, whereas several biological species that belong to the genus *Protoperidinium* have been associated with cysts belonging to different cyst-defined genera (e.g. *Brigantedinium, Quinquecuspis, Selenopemphix*, etc.) (e.g. Fensome et al. 1993). Although there have been attempts to reconcile both nomenclatural systems (e.g. Harland 1982), no consensus has yet been reached as how to resolve this issue and here we also suggest to respect the status quo in order to avoid further confusion.

~~*4.4.*~~*4.5. Evolution of* Trinovantedinium *and* Selenopemphix *within the Peridiniales*

Previous studies have tried to elucidate evolutionary patterns based on the morphologic changes of the motile stages (e.g., Taylor 1980) or on the basis of cyst morphology (e.g., Bujak & Davies 1983). Molecular phylogenetics largely support the biological approach which focuses on variations in tabulation, and consider the Monovela group and Diplopsaloideans as ancestral to the *Protoperidinium* sensu stricto group (e.g., Liu et al. 2015a,b; Gu et al. 2015; Mertens et al. 2015). Both of these ancestral groups have not been identified in the earlier fossil record of the Peridiniales (Cretaceous – Eocene), and the cyst morphologies observed during this time period (Bujak & Davies 1983) are more similar to the cyst-based genera *Lejeunecysta, Quinquecuspis* and *Trinovantedinium*, which, based on molecular phylogenetics, belong to the *Protoperidinium* sensu stricto group (Figure 3). A reinvestigation of the fossil record is urgently needed to explain this discrepancy between the fossil record and the molecular phylogenetics, and begs the question whether preservation issues or the complex cyst identification of these relatively unknown ancestral species could be responsible, or if multigene phylogenies would also support the LSU based phylogeny (e.g., Orr et al. 2012).

Trinovantedinium boreale would presumably be the oldest *Trinovantedinium* species, as it has been observed in the late Paleocene, since all other species have Miocene or later first ~~occurrences~~ appearances (Table 1). Two other closely related species to *Trinovantedinium applanatum* and *Trinovantedinium pallidifulvum*, the cyst of *Protoperidinium divaricatum* (cyst-defined ~~based~~ name *Xandarodinium xanthum*) and the cyst of *Protoperidinium leonis* (cyst-defined ~~based~~ name *Quinquecuspis concreta*) (Figure 3) both have younger first ~~occurrences~~ appearances (Miocene ~~(~~: Matsuoka, 1992~~),~~ and Pleistocene: ~~(~~de Vernal et al., 1992~~)~~, respectively). Interestingly, the here documented *Trinovantedinium applanatum* type B shows similarities to *Trinovantedinium boreale*, although the latter has longer and fewer processes. It

Formatted: Font: Bold

Formatted: Bullets and Numbering

Formatted: Font: Not Italic

would, therefore, be important to obtain a sequence from this type B and see how it relates to the other sequences.

~~4.5.~~4.6. ~~-~~*Distribution of* Trinovantedinium pallidifulvum

T. pallidifulvum was shown in this study to be widely distributed in temperate to tropical waters (Figure 1), in surface sediment samples corresponding to SSTs of ~11.30–31.45 °C and SSSs with a range of 8.60–33.61 psu.

~~4.6.~~4.7. *Cyst wall geochemistry of* Trinovantedinium pallidifulvum

The *T. pallidifulvum* cyst wall chemistry demonstrates a composition both consistent and dissimilar with other known heterotrophic dinoflagellates (Figure 4). The greatest similarity is the evidence for nitrogen-containing functional groups in the cyst wall, which is consistent with all previously analyzed cysts from heterotrophic dinoflagellates (Bogus et al. 2014). This evidence includes several absorptions indicative of amide groups (1630, 1585, 1560, 1310, and 1255 cm^{-1}). The presence of nitrogen-containing functional groups was suggested to reflect the heterotrophy of the dinoflagellate producing the cyst (Bogus et al. 2014), with the incorporation of prey waste products (high in nitrogen groups from the breakdown of proteinaceous material) into the cyst wall. Additionally, similar to other species, there is clear evidence for alcohol groups (3340, 1140 and 1030 cm^{-1}), although the strongest series of absorptions in *T. pallidifulvum* is different. In fact, the most obvious difference in the cyst wall chemistry of *T. pallidifulvum* compared to other heterotrophic dinoflagellates is the lack of the dominant series of absorptions characteristic for polysaccharides (Bogus et al. 2014; Versteegh et al. 2012). However, absorptions at 1140 and 1030 cm^{-1} are present, indicating that sugars may still be present as part of the cyst wall. The strongest absorptions are at 890 and 850 cm^{-1}, which usually result from ring vibrations and is supported somewhat by the absorption at 1630 cm^{-1}. There is also evidence that this species has a cyst wall that contains a significant carboxylic acid/ester component (1780, 1700 cm^{-1}), which may increase the stability of the cyst wall polymer (Yang et al. 1996). This pattern has been suggested in some species of the fossil *Apectodinium* genus (Bogus et al. 2012). However, the cyst wall is not aliphatic because absorptions indicating aliphatic C-H stretching are weak, which is consistent with many dinoflagellate cysts (de Leeuw et al. 2004; Bogus et al. 2014; Versteegh et al. 2012). Therefore, the spectrum of *T. pallidifulvum* is unique to any previously analyzed species because it appears to incorporate amide groups, similar to other heterotrophic species, and contain a higher abundance of ester groups, found only in two other fossil species thus far. These results suggest that dinoflagellate cyst wall chemistry may be more diverse than previously considered and further study is required.

5. Conclusions

- We document the cyst-theca relationship for the cyst-based taxon *Trinovantedinium pallidifulvum,* and erect the species *Protoperidinium lousianensis* to describe the motile stage.
- LSU rDNA based phylogenies show the closeness of *P. lousianensis* and *P. shanghaiense*, and also of their respective cysts, *Trinovantedinium pallidifulvum* and *Trinovantedinium applanatum*.
- The genus *Trinovantedinium* is monophyletic, whilst the genus *Selenopemphix* is polyphyletic.

Formatted: Font: Bold
Formatted: Bullets and Numbering
Formatted: Font: Bold
Formatted: Bullets and Numbering
Formatted: Font: Not Bold

- *Trinovantedinium pallidifulvum* is widely distributed, and can be found at SSTs of ~11.30–31.45 °C and SSSs of 8.60–33.61 psu.
- *Trinovantedinium pallidifulvum*'s cyst wall chemistry is unique but contains amide groups, which is consistent with other heterotrophic species.

Acknowledgements

Kenneth Neil Mertens is a postdoctoral researcher of FWO Belgium. Martin J. Head is acknowledged for advice on the genus *Trinovantedinium.* Anna Godhe is thanked for providing a sample from the Kattegat. Evelyne Goubert is thanked for providing a sample from La Vilaine Bay and Jean-Pierre Debenay for samples from the Vie River estuary. We acknowledge the Scripps Institution of Oceanography (SIO) Geological Collections and in particular Alex Hangsterfer for sediment samples from the Bay of Bengal. Pieter R. Gurdebeke is thanked for providing a nice specimen of *Trinovantedinium variabile.* K.N.M. and A.M.P. thank Anne de Vernal for letting us use the equipment to conduct germination experiments at GEOTOP. Sofia Ribeiro is thanked for loan of slides from Portugal. G.J.M.V. acknowledges support by the German Science Foundation (Heisenberg fellowship VE486/2). A.M.P. acknowledges the support of the Natural Science and Engineering Research Council of Canada (NSERC). Support for ship time for Gulf of Mexico specimens was provided by the National Oceanic and Atmospheric Administration, Center for Sponsored Coastal Ocean Research, under awards NA06OP0528 and NA09NOS4780204 to Louisiana Universities Marine Consortium and awards NA06OP0529 and NA09NOS4780230 to Louisiana State University. The crew of the R/V *Pelican* is thanked for assistance with sample collection. Martin J. Head and an anonymous reviewer are thanked for remarks that significantly improved the manuscript.

Author biographies

Kenneth Neil Mertens is a ~~postdoctoral~~ permanent researcher at ~~Ghent University, Belgium~~Ifremer, LER BO, Concarneau, France. He received his Ph.D. in 2009 from Ghent University. His research interests are the taxonomy, evolution, phylogeny and biogeography of dinoflagellates, and the palaeoceanographical application of dinoflagellate cysts, particularly in the Quaternary and Neogene.

Haifeng Gu is a Professor at Third Institute of Oceanography, China. He received his Ph.D. in 2007 from Ocean University of China. His research interests are taxonomy and evolution of dinoflagellates.

Yoshihito Takano is a postdoctoral researcher at National Research Institute of Fisheries Science, Fisheries Research Agency, Yokohama, Japan. He received his Ph.D. in 2006 from Hokkaido University. His research interests are taxonomy and evolution of dinoflagellates.

Andrea Price is a PhD candidate in the Department of Geography at McGill University. She recieved her BSc Honours and MSc in Earth and Ocean Sciences at the University of Victoria. Her main research interests include using dinoflagellate cysts as indicators of water quality in North American estuaries, the seasonality of cyst production, and the use of cysts in Quaternary paleoceanographic studies.

~~Dr.~~ Vera Pospelova is an Associate Professor at the School of Earth and Ocean Sciences (SEOS), University of Victoria. She received her Honours BSc in Geology from ~~the~~ Novosibirsk University (Russia) and PhD in Physical Geography from McGill University (Canada). Vera's research interests include: taxonomy of late Quaternary dinoflagellate cysts; cyst production, ecology, and seasonal dynamics in coastal waters; applications of dinoflagellate cysts as indicators of water quality conditions, with the emphasis on pollution and eutrophication in North American estuaries, as well as paleoceanographic reconstructions using sedimentary archives.

Kara Bogus is a staff scientist with the International Ocean Discovery Program (IODP) at Texas A&M University (College Station, TX, USA). She earned her PhD (marine geosciences) from the University of Bremen (Bremen, Germany). Her research interests include using organic-walled dinoflagellate cysts in paleoceanographic studies, cyst wall chemical composition and its application both to environmental reconstructions and diagenesis of sedimentary organic carbon.

Gerard Versteegh combines organic geochemistry, palynology and palaeobotany to assess organic matter degradation, and, through this, to elucidate present and past environment and evolution. In 1995 received his PhD in Biology at Utrecht University on palynology and the onset of Northern Hemisphere ~~Glaciations~~glaciations. He e~~E~~xpanded his expertise with organic geochemistry at the Netherlands Institute for Sea Research. At the Université de Lille 1, France he was an invited Professor in 2007 and 2008 and obtained a prestigious Heisenberg Fellowship from the German Science Foundation in 2009. Currently he is at the Alfred-Wegener-Institute in Bremerhaven and the Centre for Marine Environmental Research, Bremen University. His interests include the macromolecular composition of palynomorphs, selective degradation of organic matter, the Paleozoic terrestrialisation, (sub)recent Mediterranean environmental change, proxy development, lipids, acritarchs and dinoflagellates.

Fabienne Marret is a micropalaeontologist by training, with research interest in the field of Quaternary palaeoceanography and palaeoecology. She received her Ph.D. in 1994 from the University of Bordeaux, France. She studies marine sediments from around the world to interpret past environmental changes, based on vegetation tracers (pollen grains) and sea-surface conditions (dinoflagellate cysts). She is particularly interested in the causes of abrupt climate changes in the past, from the tropics to the poles.

R. Eugene Turner is a faculty member at Louisiana State University. He received his Ph.D. in 1974 from the University of Georgia, USA. His research interests include coastal oceanography and wetlands.

Nancy Rabalais is Executive Director and Professor of the Louisiana Universities Marine Consortium in Chauvin, Louisiana. Since the mid-1980s, Rabalais has been the driving force behind identifying and characterizing the dynamics of the large hypoxic region in the Gulf of Mexico, which receives excess nutrients from the Mississippi River. She serves on numerous boards and panels for federal agencies and national organizations. She has received numerous awards, most recently the John D. & Catherine T. MacArthur 'genius' award (2012). She graduated with a Ph.D. from the University of Texas in 1983.

Kazumi Matsuoka is a Professor Emeritus at Nagasaki University. ~~After retiring in~~Although retired since 2013, he continues scientific ~~works in~~research on fossil and modern dinoflagellates in particular cyst-motile form relationships of both naked and thecate dinoflagellates.

References

Adl SM, Simpson AGB, Farmer MA, Andersen RA, Anderson OR, Barta JR, Bowser SS, Brugerolle G, Fensome RA, Fredericq S, et al. 2005. The new higher level classification of Eukaryotes with emphasis on the taxonomy of Protists. J Eukaryot Microbiol. 52: 399–451.

Artzner DG, Dörhöfer G. 1978. Taxonomic note: *Lejeunecysta* nom. nov. pro *Lejeunia* Gerlach 1961 emend. Lentin and Williams 1976 - dinoflagellate cyst genus. Can J Bot 56: 1381–1382.

Baldwin RP. 1987. Dinoflagellate resting cysts isolated from sediments in Marlborough Sounds, New Zealand. New Zeal Mar Fresh. 21: 543–553.

Balech E. 1974. El Genero "*Protoperidinium*" Bergh, 1881 (*Peridinium* Ehrenberg, 1831, partim). Revista Mus Argent Ci Nat, Bernardino Rivadavia Inst Nac Invest Ci Nat Bot. 4: 1–79.

Balech E. 1988. Los dinoflagellados del Atlántico Sudoccidental. Pub Esp Inst Español Oceanografía 1: 1–310.

Benedek PN. 1972. Phytoplanktonten aus dem Mittel- und Oberoligozän von Tönisberg (Niederrheingebiet). Palaeontogr Abt B 137: 1–71.

Bergh RS. 1881. Der Organismus der Cilioflagellaten. Eine phylogenetische Studie. Gegenbaurs Morpholog Jahrb. 7: 177–288.

Boc A, Diallo AB, Makarenkov V. 2012. T-REX: a web server for inferring, validating and visualizing phylogenetic trees and networks. Nucleic Acids Res. 40: W573–W579.

Boessenkool K, Van Gelder M-J, Brinkhuis H, Troelstra SR. 2001. Distribution of organic-walled dinoflagellate cysts in surface sediments from transects across the Polar Front offshore southeast Greenland. J Quaternary Sci. 16: 661–666.

Bogus K, Harding IC, King A, Charles AK, Zonneveld K, Versteegh, GJM. 2012. The composition of species of the *Apectodinium* complex (Dinoflagellata). Rev Palaeobot Palynol. 183: 21–31.

Bogus K, Mertens KNM, Lauwaert J, Harding IC, Vrielinck H, Zonneveld K, Versteegh, GJM. 2014. Differences in the chemical composition of organic-walled dinoflagellate resting cysts from phototrophic and heterotrophic dinoflagellates. J Phycol. 50: 254–266.

Bolch CJS. 1997. The use of polytungstate for the separation and concentration of living dinoflagellate cysts from marine sediments. Phycologia 37: 472–478.

Formatted: Font: Italic

Formatted: Font: Italic

Bradford MR. 1977. New species attributable to the dinoflagellate cyst genus *Lejeunia* Gerlach, 1961 emend. Lentin and Williams 1975. Grana 16: 45–59.

Bringué M, Pospelova V, Pak D. 2013. Seasonal production of organic-walled dinoflagellate cysts in an upwelling system: a sediment trap study from the Santa Barbara Basin, California. Mar Micropaleontol. 100: 34–51.

Bujak JP. 1984. Cenozoic dinoflagellate cysts and acritarchs from the Bering Sea and northern North Pacific, D.S.D.P. Leg 19. Micropaleontology 30: 180–212.

Bujak JP, Davies EH. 1983. Modern and fossil Peridiniineae. AASP Contribution Series 13: 1–204.

Bütschli O. 1885. Erster Band. Protozoa. 3. Unterabtheilung (Ordnung) Dinoflagellata. In: Dr. H.G. Bronn's Klassen und Ordnungen des Thier-Reichs, wissenschaftlich dargestellt in Wort und Bild. C.F. Leipzig und Heidelberg: Winter'sche Verlagshandlung; p. 906–1029.

Cárdenas G, Cabrera G, Taboada E, Miranda SP. 2004. Chitin characterization by SEM, FTIR, XRD, and 13C cross polarization/mass angle spinning NMR. J Appl Polym Sci. 93: 1876–1885.

Cho H-J, Kim C-H, Moon C-H, Matsuoka K. 2003. Dinoflagellate cysts in recent sediments from the southern coastal waters of Korea. Bot Mar. 46: 332–337.

Colthup NB, Daly LH, Wiberly SE. 1990. Introduction to Infrared and Raman Spectroscopy. London: Academic Press Limited.

Daugbjerg N, Hansen G, Larsen J, Moestrup Ø. 2000. Phylogeny of some of the major genera of dinoflagellates based on ultrastructure and partial LSU rDNA sequence data, including the erection of three new genera of unarmoured dinoflagellates. Phycologia 39: 302–317.

de Leeuw JW, Versteegh GJM, van Bergen PF. 2006. Biomacromolecules of algae and plants and their fossil analogues. Plant Ecol. 182: 209–233.

De Schepper S, Head MJ, Louwye S. 2009. Pliocene dinoflagellate cyst stratigraphy, palaeoecology and sequence stratigraphy of the Tunnel-Canal Dock, Belgium. Geol Mag 146: 92–112.

de Vernal A, Londeix L, Mudie PJ, Harland R, Morzadec-Kerfourn M-T, Turon J-L, Wrenn JH. 1992. Quaternary organic-walled dinoflagellate cysts of the North Atlantic Ocean and adjacent seas: ecostratigraphy and biostratigraphy. In: Head MJ, Wrenn JH, editors. Neogene and Quaternary dinoflagellate cysts and acritarchs. Dallas, Texas: American Association of Stratigraphic Palynologists Foundation; p. 289–328.

de Verteuil L, Norris G. 1992. Miocene Protoperidiniacean dinoflagellate cysts from the Maryland and Virginia coastal plain. In: Head MJ, Wrenn JH, editors. Neogene and Quaternary

dinoflagellate cysts and acritarchs. Dallas, Texas: American Association of Stratigraphic Palynologists Foundation; p. 391–430.

Faust MA. 2006. Creation of the subgenus *Testeria* Faust *subgen. nov. Protoperidinium* Bergh from the SW Atlantic Ocean: *Protoperidinium novella* sp. nov. and *Protoperidinium concinna* sp. nov. Dinophyceae. Phycologia 45: 1–9.

Fensome RA, Taylor FJR, Norris G, Sarjeant WAS, Wharton DI, Williams GL. 1993. A classification of fossil and living dinoflagellates. Micropaleontology Special Publication 7: 1–245.

Fukuyo Y, Takano H, Chihara M, Matsuoka K. 1990. Red tide organisms in Japan-An illustrated taxonomic guide. In: Fukuyo Y, Takano H, Chihara M, Matsuoka, editors. Tokyo, Japan: Uchida Rokakuho Co. Ltd. (In Japanese/English); 407 p.

Furio EE, Matsuoka K, Mizushima K, Baula I, Chan KW, Puyong A, Srivilai D, Sidharta, BR, Fukuyo Y. 2006. Assemblage and geographical distribution of dinoflagellate cysts in surface sediments of coastal waters of Sabah, Malaysia. Coastal Marine Science 30: 62–73.

Gómez F. 2012. A checklist and classification of living dinoflagellates (Dinoflagellata, Alveolata). CICIMAR Oceánides 27: 65–140.

Gribble KE, Anderson DA. 2006. Molecular phylogeny of the heterotrophic dinoflagellates, *Protoperidinium*, *Diplopsalis* and *Preperidinium* (Dinophyceae), inferred from large subunit rDNA. J Phycol 42: 1081–1095.

Gu H, Liu T, Mertens KN. 2015. Cyst-theca relationship and phylogenetic positions of *Protoperidinium* (Peridiniales, Dinophyceae) species of the sections *Conica* and *Tabulata*. Phycologia 54: 49–66.

Haeckel E. 1894. Systematische Phylogenie. Entwurf eines natürlichen Systems der Organismen auf Grund ihrer Stammesgeschichte. 1. Theil: Systematische Phylogenie der Protisten und Pflanzen: p. I–XV + 1–400, Georg Reimer (Berlin).

Hall TA. 1999. BioEdit: a user-friendly biological sequence alignment editor and analysis program for Windows 95/98/NT. pp. 95–98.

Harland R. 1977. Recent and Late Quaternary (Flandrian and Devensian) dinoflagellate cysts from marine continental shelf sediments around the British Isles. Palaeontogr Abt B 164: 87–126.

Harland R. 1982. A review of recent and quaternary organic-walled dinoflagellate cysts of the genus *Protoperidinium*. Palaeontology 25: 369–397.

~~Head MJ, Norris G, Mudie PJ. 1989. 26. New species of dinocysts and a new species of acritarch from the upper Miocene and lowermost Pliocene, ODP Leg 105, Site 646, Labrador Sea. In: Srivastava SP, Arthur M, Clement B, et al., editors. Ocean Drilling Program, Proceedings, Scientific Results, Leg 105, p. 453–466.~~

Head MJ. 1993. Dinoflagellates, sporomorphs and other palynomorphs from the Upper Pliocene St. Erth Beds of Cornwall, southwestern England. J Paleo. Memoir 31: 1–62.

Head MJ. (Ed.) 1994. A forum on Neogene and Quaternary dinoflagellate cysts: the edited transcript of a round table discussion held at the Third Workshop on Neogene and Quaternary Dinoflagellates; with taxonomic appendix. Palynology 17: 201–239. [Imprinted 1993]

Head MJ, Norris G, Mudie PJ. 1989. 26. New species of dinocysts and a new species of acritarch from the upper Miocene and lowermost Pliocene, ODP Leg 105, Site 646, Labrador Sea. In: Srivastava SP, Arthur M, Clement B, et al., editors. Ocean Drilling Program, Proceedings, Scientific Results, Leg 105, p. 453–466.

Head MJ, Riding JB, Eidvin T, Chadwick RA. 2004. Palynological and foraminiferal biostratigraphy of (Upper Pliocene) Nordland Group mudstones at Sleipner, northern North Sea. Mar Petrol Geol 21: 277–297.

Hoppenrath M, Elbrächter M, Drebes G. 2009. Marine Phytoplankton. Selected Microphytoplankton Species from the North Sea around Helgoland and Sylt. Kleine Senckenberg-Reihe 49, 264 pp.

Jiménez-Moreno G, Head MJ, Harzhauser M. 2006. Early and Middle Miocene dinoflagellate cyst stratigraphy of the Central Paratethys, Central Europe. J Micropal 25: 113–139.

Jörgensen E. 1912. Bericht über die von der schwedischen Hydrographisch- Biologischen Kommission in den schwedischen Gewässern in den Jahren 1909-1910 eingesammelten Planktonproben. Svenska Hydrogr-Biol Komm Skr. 4: 1–20.

Katoh K, Kuma K, Toh H, Miyata T. 2005. MAFFT version 5: improvement in accuracy of multiple sequence alignment. Nucleic Acids Res. 33: 511–518.

Kawami H, Matsuoka K. 2009. A new cyst-theca relationship for *Protoperidinium parthenopes* (Peridiniales, Dinophyceae). Palynology 33: 11–18.

Kawami H, van Wezel R, Koeman RPT, Matsuoka K. 2009. *Protoperidinium tricingulatum* sp. nov. (Dinophyceae), a new motile form of a round, brown, and spiny dinoflagellate cyst. Phycol Res. 57: 259–267.

Kojima N, Seto K, Takayasu K, Nakamura M. 1994. Dinoflagellate cysts assemblage found in the surface sediments of Lake Nakaumi, Western Japan. Laguna 1: 45–51.

Krepakevich A, Pospelova V. 2010. Tracing the influence of sewage discharge on coastal bays of Southern Vancouver Island (BC, Canada) using sedimentary records of phytoplankton. Cont Shelf Res. 30: 1924–1940.

Lewis J, Dodge JD, Tett P. 1984. Cyst-theca relationships in some *Protoperidinium* species (Peridiniales) from Scottish sea lochs. Journal of Micropalaeontology 3: 25–34.

Lewis J, Dodge JD. 1987. The cyst-theca relationship of *Protoperidinium americanum* (Gran & Braarud) Balech. Journal of Micropalaeontology 6: 113–121.

Li Z, Matsuoka K, Shin HH, Kobayashi S, Shin K, Lee T, Han M-S, 2015. *Brigantedinium majusculum* is the cyst of *Protoperidinium sinuosum* (Protoperidiniaceae, Dinophyceae). Phycologia 54: 517–529.

Liu T, Gu H, Mertens KN, Lan D. 2014. A new dinoflagellate species *Protoperidinium haizhouense* sp. nov. (Peridiniales, Dinophyceae), its cyst-theca relationship and phylogenetic position within the *Monovela* group. Phycol Res. 62: 109–124.

Liu T, Mertens KN, Ribeiro S, Ellegaard M, Matsuoka H, Gu H. 2015a. Cyst-theca relationships and phylogenetic positions of Peridiniales (Dinophyceae) with two anterior intercalary plates, with description of *Archaeperidinium bailongense* n. sp. and *Protoperidinium fuzhouense* n. sp. Phycol Res. 63: 134–151.

Liu T, Mertens KN, Gu H. 2015b. Cyst-theca relationship and phylogenetic positions of the diplopsalioideans (Peridiniales, Dinophyceae), with description of *Niea* and *Qia* gen. nov. Phycologia 54: 210–232.

Louwye S, Mertens KN, Vercauteren D. 2008. New dinoflagellate cysts from the Miocene of the Porcupine Basin, offshore southwest Ireland. Palynology 32: 131–142.

Matsuoka K. 1982. *Protoperidinium pentagonum* (Gran) Balech. In: the working party in taxonomy in the Akashiwo Kenyukai, editors. Synopsis of Red-tide organisms. Sheet no. 108 [In Japanese].

Matsuoka K. 1987. Organic-walled dinoflagellate cysts from surface sediments of Akkeshi Bay and Lake Saroma, North Japan. Bulletin Faculty of Liberal Arts, Nagasaki University (Natural Science) 28: 35–123.

Matsuoka K. 1992. Peridiniacean cyst genus *Xandarodinium* in the Miocene Kaminoyama Formation in the western part of Zao Volcano, Yamagata, north Japan. In: Ishizaki K, Saito T., editors. Centenary of Japanese Micropaleontology. Tokyo, Japan: Terra Scientific Publishing Company; p.449-455.

Matsuoka K, Head MJ. 2013. Clarifying cyst–motile stage relationships in dinoflagellates. In: Lewis JM, Marret F, Bradley L., editors. Biological and Geological Perspectives of

Dinoflagellates. London: The Micropalaeontological Society, Special Publications. Geological Society, p. 325–350.

Matsuoka K, Kawami H, Nagai S, Iwataki M, Takayama H. 2009. Re-examination of cyst-motile relationships of *Polykrikos kofoidii* Chatton and *Polykrikos schwartzii* Bütschli (Gymnodiniales, Dinophyceae). Rev Palaeobot Palynol 154: 79–90.

Matsuoka K, Joyce LB, Kotani Y, Matsuyama Y. 2003. Modern dinoflagellate cysts in hypertrophic coastal waters of Tokyo Bay, Japan. J Plankton Res. 25: 1461–1470.

Mertens KN, Yamaguchi A, Kawami H, Ribeiro S, Leander BS, Price AM, Pospelova, V, Ellegaard, M, Matsuoka K. 2012a. *Archaeperidinium saanichi* sp. nov.: A new species based on morphological variation of cyst and theca within the *Archaeperidinium minutum* Jörgensen 1912 species complex. Mar Micropaleontol. 96: 48–62.

Mertens KN, Bringué M, Van Nieuwenhove N, Takano Y, Pospelova V, Rochon A, de Vernal A, Radi T, Dale B, Patterson RT, Weckström K, Andrén E, Louwye S, Matsuoka K. 2012b. Process length variation of the cyst of the dinoflagellate *Protoceratium reticulatum* in the North Pacific and Baltic-Skagerrak region: calibration as an annual density proxy and first evidence of pseudo-cryptic speciation. J Quaternary Sci. 27: 734–744.

Mertens KN, Yamaguchi A, Takano Y, Pospelova V, Head MJ, Radi T, Pieńkowski A, de Vernal A, Kawami H, Matsuoka K. 2013. A new heterotrophic dinoflagellate from the Northeastern Pacific, *Protoperidinium fukuyoi*: cyst-theca relationship, phylogeny, distribution and ecology. J Eukaryot Microbiol. 60: 545–563.

Mertens KN, Takano Y, Yamaguchi A, Gu H, Bogus K, Kremp A, Bagheri S, Matishov G, Matsuoka K. 2015. The molecular characterization of the enigmatic dinoflagellate *Kolkwitziella acuta* reveals an affinity to the *Excentrica* section of the genus *Protoperidinium.* Syst Biodivers. doi:10.1080/14772000.2015.1078855.

Nehring S. 1997. Dinoflagellate resting cysts from German coastal sediments. Bot Mar. 40: 307–324.

Orr RJS, Murray SA, Stüken A, Rhodes L, Jakobsen KS. 2012. When naked became armored: An eight-gene phylogeny reveals monophyletic origin of theca in dinoflagellates. PloS one 7: e50004.

Pascher A. 1914. Über Flagellaten und Algen. Berichte der Deutschen Botanischen Gesellschaft 32: 136–160.

Posada D. 2008. jModelTest: phylogenetic model averaging. Mol Biol Evol. 25: 1253–1256.

Pospelova V, Chmura GL, Walker HA. 2004. Environmental factors influencing spatial distribution of dinoflagellate cyst assemblages in shallow lagoons of southern New England (USA). Rev Palaeobot Palynol. 128:7–34.

Formatted: Font: Italic

Formatted: Font: Italic

Pospelova V, de Vernal A, Pedersen TF. 2008. Distribution of dinoflagellate cysts in surface sediments from the northeastern Pacific Ocean (43–25 degrees N) in relation to sea-surface temperature, salinity, productivity and coastal upwelling. Mar Micropaleontol. 68: 21–48.

Price AM, Pospelova V. 2011. High-resolution sediment trap study of organic-walled dinoflagellate cyst production and biogenic silica flux in Saanich Inlet (BC, Canada). Mar Micropaleontol. 80: 18–43.

Radi T, de Vernal A. 2004. Dinocyst distribution in surface sediments from the northeastern Pacific margin (40-60°N) in relation to hydrographic conditions, productivity and upwelling. Rev Palaeobot Palynol. 128: 169–193.

Reid P. 1977. Peridiniacean and glenodiniacean dinoflagellate cysts from the British Isles. Nova Hedwigia 29: 429–463.

Ribeiro S, Lundholm N, Amorim A, Ellegaard M. 2010. *Protoperidinium minutum* (Dinophyceae) from Portugal: cyst-theca relationship and phylogenetic position on the basis of single-cell SSU and LSU rDNA sequencing. Phycologia 49: 48–63.

Rochon A, de Vernal A, Turon J-L, Matthiessen J, Head MJ. 1999. Distribution of recent dinoflagellate cysts in surface sediments from the North Atlantic Ocean and adjacent seas in relation to sea-surface parameters. AASP Contribution Series, 35, 146 pp.

Ronquist F, Huelsenbeck JP. 2003. MrBayes 3: Bayesian phylogenetic inference under mixed models. Bioinformatics 19: 1572–1574.

Sarai C, Kawami H, Matsuoka K. 2013. Two new species formally attributed to *Protoperidinium oblongum* (Aurivillius) Park et Dodge (Peridiniales, Dinophyceae): Evidence from cyst incubation experiments. Rev Palaeobot Palynol. 192: 103–118.

Scholin CA, Herzog M, Sogin M, Anderson DM. 1994. Identification of group- and strain-specific genetic markers for globally distributed *Alexandrium* (Dinophyceae). II. Sequence analysis of a fragment of the LSU rRNA gene. J Phycol. 30: 999–1011.

Shin HH, Yoon YH, Kim Y-O, Matsuoka K. 2011. Dinoflagellate Cysts in Surface Sediments from Southern Coast of Korea. Estuaries and Coasts 34: 712–725.

Soliman A, Ćorić S, Head MJ, Piller W, El Beialy SY, 2012. Lower and Middle Miocene biostratigraphy, Gulf of Suez, Egypt, based on dinoflagellate cysts and calcareous nannofossils. Palynology 36: 1–42.

Stamatakis A. 2006. RAxML-VI-HPC: maximum likelihood-based phylogenetic analyses with thousands of taxa and mixed models. Bioinformatics 22: 2688–2690.

Taylor F. 1980. On dinoflagellate evolution. BioSystems 13: 65–108.

Formatted: Font: 12 pt

Formatted: Font: 12 pt

Formatted: Font: 12 pt

Verleye T, Pospelova V, Mertens KN, Louwye S. 2011. The geographical distribution and (palaeo)ecology of *Selenopemphix undulata* sp. nov., a new late Quaternary dinoflagellate cyst from the Pacific Ocean. Mar Micropaleontol.78: 65–83.

Versteegh GJM, Blokker P, Bogus K, Harding IC, Lewis J, Oltmanns S, Rochon A, Zonneveld KAF. 2012. Flash pyrolysis and infrared spectroscopy of cultured and sediment derived *Lingulodinium polyedrum* (Dinoflagellata) cyst walls. Org Geochem. 43: 92–102.

Wall D, Dale B. 1968. Modern dinoflagellate cysts and evolution of the Peridiniales. Micropaleontology 14: 265–304.

Wang Z, Matsuoka K, Qi Y, Chen J. 2004. Dinoflagellate cysts in recent sediments from Chinese coastal waters. Marine Ecology 25: 289–311.

Yamaguchi A, Kawamura H, Horiguchi T. 2006. A further phylogenetic study of the heterotrophic dinoflagellate genus, *Protoperidinium* (Dinophyceae) based on small and large subunit ribosomal RNA gene sequences. Phycol Res. 54: 317–329.

Yamaguchi A, Kawamura H, Horiguchi T. 2007. The phylogenetic position of an unusual *Protoperidinium* species, *P. bipes* (Peridiniales, Dinophyceae), based on small and large subnit ribosomal RNA gene sequences. Phycologia 46: 270–276.

Yamaguchi A, Hoppenrath M, Pospelova V, Horiguchi T, Leander BS. 2011. Molecular phylogeny of the marine sand-dwelling dinoflagellate *Herdmania litoralis* and an emended description of the closely related planktonic genus *Archaeperidinium* Jörgensen. Eur J Phycol. 46: 98–112.

Yang CQ, Xu Y, Wang D. 1996. FT-IR spectroscopy study of the polycarboxylic acids used for paper wet strength improvement. Ind Eng Chem Res. 35: 4037–4042.

989

Tables

Table 1. List of species belonging to the genus *Trinovantedinium*, their biostratigraphical ranges and dimensions.

Species name	Biostratigraphical range	Length (excluding processes) (µm)	Width (excluding processes) (µm)	Length of processes (µm)	Measurements from
Trinovantedinium applanatum (Bradford 1977) Bujak and Davies 1983	middle Pleistocene (Mudie 1989) - recent (see Rochon et al. 1999 for remarks)	53—87	47—74	max 5	Bradford 1977
		54—80	54—80	max 5—7	Reid 1977
Trinovantedinium sterthense Head 1993a	~~late Pliocene~~early Pleistocene (Head 1993a)	41(50.0)61	45(49.6)53	4.5(5.5)7.0	Head 1993a
Trinovantedinium variabile (Bujak 1984) de Verteuil and Norris 1992	late Miocene (Bujak 1984) — recent (e.g., Radi & de Vernal 2004; Price & Pospelova 2011)	45—53	44—50	4—6.5	Bujak 1984
Trinovantedinium harpagonium de Verteuil and Norris 1992	middle Miocene (~~late Miocene (de Verteuil & Norris 1992~~Jiménez-Moreno et al. 2006) — late Pliocene (De Schepper et al. 2009)	52(60)78	48(59)68	8—16	de Verteuil & Norris 1992
Trinovantedinium glorianum (Head et al. 1989) de Verteuil and Norris 1992	early Miocene (Louwye et al. 2007) — early Pleistocene (Head et al. 2004)	58(68)73	52(63)70	2—3	de Verteuil & Norris 1992
Trinovantedinium ferrugnomatum de Verteuil and Norris 1992	late Miocene (de Verteuil & Norris 1992) — early Pliocene (De Schepper et al. 2009)	30(39)55	30(39)48	3—6	de Verteuil & Norris 1992
Trinovantedinium papula de Verteuil and Norris 1992	late Miocene (de Verteuil & Norris 1992)	50(65)75	48(57)70	3—6	de Verteuil & Norris 1992
Trinovantedinium pallidifulvum Matsuoka 1987	mid Miocene (de Verteuil & Norris 1992[1]) — recent (Matsuoka 1987)	52.2—70.8	56.0—63.4	2.5	Matsuoka 1987
		43.0(58.5)68.4	46.3(56.5)63.9	1.1(1.8)2.7	This study
Trinovantedinium henrietii Louwye et al. 2008	mid Miocene (Louwye et al. 2008)	81(89)99	61(75)84	5(7)10	Louwye et al. 2008
Trinovantedinium? xylochoporum de Verteuil and Norris 1992	lower Miocene (Soliman et al. 2012) — middle Miocene (Jiménez-Moreno et al., 2006)~~mid Miocene (de Verteuil & Norris 1992)~~	36(51)66	38(45)62	8-20	de Verteuil & Norris 1992
Trinovantedinium boreale Bujak 1984	late Paleocene — late Oligocene (Kurita & Matsuoka 1993; see Head 1994 for discussion)	42-65	42-63	7-15	Bujak 1984

[1]Our interpretation of the "undefined protoperidiniacean species" depicted in de Verteuil & Norris, plate 2, figs. 9—12.

Formatted: French (France)

Formatted: English (U.K.)

Formatted: English (U.S.)

Formatted: English (U.K.)

Formatted: Font: Not Italic

Formatted: English (U.K.)

Table 2. Sampling stations with details on the collection site, relative abundance (%) and how the sample was used in this study.

Station	Location	Latitude (°N)	Longitude (°E)	Water depth (m)	Sampling data	Salinity (psu)	Temperature (°C)	Type of core	Sampled by*	Relative abundance (%)	Notes
Heslwall, Dee Estuary	UK	53,32	-3,12	0	6/02/14	NA	NA	Hand sampling	FM	NA	Germination experiment
Wadden Sea st . 1	Northern Germany	53,72	7,97	0	29/02/12	NA	NA	Hand sampling	GV, KZ, KNM	NA	Germination experiment
Vinga SW	Kattegat	57,55	11,53	77,5	1994	NA	NA	Boxcore	AG	NA	Palynological study
BV3	La Vilaine Bay, France	47,48	-2,44	6	1/04/10	NA	NA	Boxcore	EG	NA	Palynological study
C6B	Gulf of Mexico	28,87	-90,47	18,4	28/07/08	22,17	30,54	Boxcore	GT, NR	0,8	Palynological study
E2A	Gulf of Mexico	28,74	-91,25	15,2	28/07/08	16,14	29,7	Boxcore	GT, NR	0,6	Palynological study
G3	Gulf of Mexico	28,98	-92,00	20,2	28/07/08	21,51	30,45	Boxcore	GT, NR	0,9	Palynological study
J4	Gulf of Mexico	29,29	-93,08	15	25/07/08	27,99	30,52	Boxcore	GT, NR	0,8	Palynological study
A'2	Gulf of Mexico	29,09	-89,50	11,2	27/07/14	8,60	31,45	Boxcore	GT, NR	0,3	Palynological study
A'3	Gulf of Mexico	29,03	-89,53	13,2	27/07/14	13,60	30,99	Boxcore	GT, NR	1,7	Palynological study
A'4	Gulf of Mexico	28,98	-89,57	33,7	27/07/14	15,15	30,90	Boxcore	GT, NR	0,6	Palynological study
A'5	Gulf of Mexico	28,95	-89,58	63,9	27/07/14	17,73	30,19	Boxcore	GT, NR	1,7	Palynological study
A2	Gulf of Mexico	29,24	-89,75	13,5	28/07/14	25,00	30,00	Boxcore	GT, NR	1,2	Palynological study
A5	Gulf of Mexico	29,07	-89,75	30,5	28/07/14	25,30	29,70	Boxcore	GT, NR	1,2	Palynological study
A7	Gulf of Mexico	28,94	-89,75	53,20	28/07/14	24,70	29,90	Boxcore	GT, NR	2,0	Germination experiment / Palynological study
B4	Gulf of Mexico	29,03	-90,12	18,5	28/07/14	28,09	29,55	Boxcore	GT, NR	3,8	Palynological study
C6C	Gulf of Mexico	28,87	-90,49	19,80	28/07/14	23,40	29,40	Boxcore	GT, NR	1,8	Single-cell PCR / Palynological study
D3	Gulf of Mexico	28,72	-90,83	17,8	29/07/14	15,05	30,83	Boxcore	GT, NR	2,4	Palynological study
F0	Gulf of Mexico	29,27	-91,62	8,0	31/07/14	23,20	31,30	Boxcore	GT, NR	3,7	Palynological study
F3	Gulf of Mexico	28,88	-91,62	19,9	30/07/14	29,15	29,92	Boxcore	GT, NR	1,5	Palynological study
F6	Gulf of Mexico	28,58	-91,62	39,6	30/07/14	30,02	29,51	Boxcore	GT, NR	0,8	Palynological study
I4	Gulf of Mexico	29,18	-92,75	20,8	1/08/14	32,40	30,00	Boxcore	GT, NR	0,3	Palynological study
K4	Gulf of Mexico	29,33	-93,42	17,3	1/08/14	31,74	29,92	Boxcore	GT, NR	0,8	Palynological study
P6	Gulf of Mexico	29,00	-93,71	20,0	1/08/14	33,61	30,08	Boxcore	GT, NR	0,3	Palynological study
SR8	Lake Saroma	44,09	143,52	ca. 7	July 1980	33-33.2	0-15	TFO corer	YF	0,5	Palynological study

AK2	Akkeshi Bay, Japan	43,02	144,47	ca. 6	July 1980	32.6-33	1.5(winter)-14(summer)	TFO corer	YF	0.5-1.8	Palynological study
AB40	Ariake Sound, Japan	33,08	130,28	10,9	7/06/05	20.0-30.2	9.2-28.5	TFO corer	KM	NA	Palynological study
Tkb8	Tokyo Bay, Japan	35,27	139,45	ca.12	1/08/99	26.8-30.5	10.4-30.1	KK type corer	RV	NA	Palynological study
Nagayo-Ura	Omura Bay, Japan	32,51	129,52	11	June 2004	30.8-33.4	9.5-30.5	sediment trap	HK, KM	NA	Palynological study
YJ1	Yeoja Bay, Korea	34,42	127,31	11	May 2006	NA	NA	Scuba diver	KM, HC	NA	Palynological study
D1	Deukryang Bay, Korea	34,40	127,11	10	1/04/01	NA	NA	Gravity corer	HC	NA	Palynological study
Casino coast	Brazil	-32,12	-52,10	ca.10	7/03/97	NA	NA	TFO corer	KM	NA	Palynological study
Saanich Inlet st. S13	Vancouver Island, BC, Canada	48,75	-123,61	60	24/05/07	28,5	11,3	Petite Ponar Grab	VP	NA	Palynological study

* AG = Anna Godhe, EG = Evelyne Goubert, FM = Fabienne Marret, GV= Gerard Versteegh, GT = Gene Turner, HC = Hyun-Jin Cho, HK = Hisae Kawami, KM = Kazumi Matsuoka, KNM = Kenneth Neil Mertens, KZ = Karin Zonneveld, NR = Nancy Rabalais, RV = R/V Shirafuji-Maru, VP = Vera Pospelova, YF = Yasuo Fukuyo

1000

1001 Supplementary table 1. Sampling stations with details on latitude, longitude and water depth.

Name of station	Locality	Latitude (°N)	Longitude (°E)	Water depth (m)	Reference
Akkeshi Bay AK1	Hokkaido, Japan	43,04	144,83	25	Matsuoka 1987
Akkeshi Bay AK2	Hokkaido, Japan	43,02	144,79	25	Matsuoka 1987
Akkeshi Bay AK3	Hokkaido, Japan	42,99	144,79	25	Matsuoka 1987
Akkeshi Bay AK4	Hokkaido, Japan	42,95	144,86	25	Matsuoka 1987
Saroma lake SR8	Hokkaido, Japan	44,14	143,86	16	Matsuoka 1987
6	Lake Nakaumi, Japan	35,52	134,08	NA	Kojima et al. 1994
8	Lake Nakaumi, Japan	35,52	134,08	NA	Kojima et al. 1994
24	Lake Nakaumi, Japan	35,52	134,08	NA	Kojima et al. 1994
25	Lake Nakaumi, Japan	35,52	134,08	NA	Kojima et al. 1994
26	Lake Nakaumi, Japan	35,52	134,08	NA	Kojima et al. 1994
TKB-6	Tokyo Bay, Japan	35,50	139,83	NA	Matsuoka et al. 2003
D1	South of South Korea	34,67	127,18	10	Cho et al. 2003
4	Chinese coast	22,56	114,51	6	Wang et al. 2004
Kuala Penyu Lagoon 1	Sabah, Malaysia	5,53	115,62	NA	Furio et al. 2006
Kuala Penyu Lagoon 2	Sabah, Malaysia	5,57	115,60	NA	Furio et al. 2006
YJB1	Yeoja Bay, South Korea	34,78	127,50	NA	Shin et al. 2011
YJB2	Yeoja Bay, South Korea	34,74	127,50	NA	Shin et al. 2011
YJB3	Yeoja Bay, South Korea	34,71	127,50	NA	Shin et al. 2011
YJB4	Yeoja Bay, South Korea	34,67	127,51	NA	Shin et al. 2011
YJB6	Yeoja Bay, South Korea	34,50	127,59	NA	Shin et al. 2011
YJB8	Yeoja Bay, South Korea	34,43	127,70	NA	Shin et al. 2011
GMB3	Gamak Bay, South Korea	34,60	127,70	NA	Shin et al. 2011

Figure captions

Figure 1. Map showing locations where *Trinovantedinium pallidifulvum* was found in this study (red circles) and in previous studies (blue circles) (see Table 1 and Supplementary Table 1 for respective sample localities).

Figure 2. Drawings of *Protoperidinium louisanensis* n. sp. A). Ventral view. B). Dorsal view.

Figure 3. Molecular phylogeny. A phylogenetic tree using Bayesian inference inferred from LSU rDNA sequences based on new sequence data for *Protoperidinium louisanensis* n. sp. from the Gulf of Mexico and *Selenopemphix undulata* from Brentwood Bay, BC, Canada. The ML bootstrap support values (ML) over 50 and Bayesian posterior probabilities (PP) over 0.7 are shown at the nodes (ML/PP). The black circles indicate maximal support. Clades are labeled and marked with vertical lines on the right, with dashed lines indicating sections of the *Protoperidinium* sensu stricto clade. The scale bar represents inferred evolutionary distance in changes/site. New sequences obtained in this study are indicated in bold font.

Figure 4. *Trinovantedinium pallidifulvum* (German Wadden Sea) cyst wall FTIR spectrum in comparison with other cysts produced by heterotrophic dinoflagellates. The spectra from *D. caperatum*, *Brigantedinium* sp., cysts of *Polykrikos kofoidii* sensu Matsuoka et al. (2009) and *Polykrikos schwartzii* sensu Matsuoka et al. (2009) are modified from Bogus et al. (2014).

Plate captions

Plate 1. Figures 1–9. Different views of single specimen of motile stage of *Protoperidinium louisanensis* germinated from cyst depicted in Figures 10–15, and isolated from the Northern Gulf of Mexico. 1. General shape of cell. 2. Ventral view. 3. Lateral view. 4. Dorsal view showing the second intercalary plate (2a). 5. Lateral view. 6. Lateral view. 7. Ventral view showing sulcal area. 8. Dorsal view. 9. Ventral view of hypotheca. Figures 10–15. Cyst stage of *Protoperidinium louisanensis*, corresponding to *Trinovantedinium pallidifulvum,* with motile stage depicted in Figures 1–9. 10. Ventral view. 11. Cross section. 12. Dorsal view showing operculum. 13. Peritabular distribution of processes. 14-15. Ventral view showing process distribution on the hypotheca. All scale bars = 10 µm.

Plate 2. Figures 1–9. Motile stage of *Protoperidinium louisanensis* germinated from cyst depicted in Figures 10-15, isolated from the Northern Gulf of Mexico. 1. Cross section showing general shape and cell contents. 2. Ventral view. 3. Ventral view showing shape of the first apical plate. 4. Focus on the apical pore. 5. Dorsal view showing shape of second intercalary plate (2a). 6. Lateral view. 7. Ventral view showing sulcal area. 8. Dorsal view. 9. View of dorsal side of hypotheca. Figures 10–15. Cyst stage of *Protoperidinium louisanensis*, corresponding to *Trinovantedinium pallidifulvum,* with motile stage depicted in Figures 1–9. 10. General shape of cyst. 11. Ventral view showing peritabular distribution of processes. 12. Ventral view showing presence of 2 flagellar scars. 13. Lateral view. 14. Dorsal view showing operculum. 15. Dorsal view of hypotheca showing presence of striations on this specimen. All scale bars = 10 µm.

Plate 3. Figures 1–12. *Trinovantedinium pallidifulvum* from German Wadden Sea. 1–3. Cyst with cell contents from St. 1. 4–8. Different orientations of germinated specimen. 9–12. Other specimen). 9. Apical pore. Figures 13–16. Holotype of *Trinovantedinium pallidifulvum*. Slide no. AK2–2 (87.4/27.6); Sample no. AK2, ~~Recent~~ modern sediment in Akkeshi Bay, Hokkaido, North Japan (Matsuoka 1987). All scale bars = 10 µm.

Plate 4. Figures 1–12. *Trinovantedinium applanatum*. 1-4. High focus to low focus of single specimen from 11–12 cm depth in core po287-39-1B (37.75°N, 8.87°W, 92 m water depth, Mira, Portugal). 5–6, 8–10. Different orientations of single specimen isolated from the German Wadden Sea (location shown in Table 2). 7. Other specimen from the German Wadden Sea. 11–13. Scanning electron microscope photographs of specimens isolated from Vie River st. 10 (46.70°N, 1.94°W, France). All scale bars = 10 µm.

Plate 5. *Trinovantedinium applanatum* type A and B occurring in recent sediments. 1–2, 5–7. Different views of single specimen from Type A from station 1 (32.93°N, 129.86°E, 11.1 m water depth, Omura Bay, Japan). 3. Type A from Red Sea (va01-200P, 0-5 cm depth, 16.67°N, 41.32°E, , 84 m water depth). 4. Specimen from 1–2 cm core depth from core CIRCE03AR 25P (15.30°N, 83.39°E, 3145m water depth, Bay of Bengal). 8–9. Type B from sample 11B (35.87°W, 64.11°N, 1318 m water depth, offshore Greenland, Boessenkool et al. 2001). 10. Type B from sample 1B (60.02°N, 11.76°W, water depth unknown, offshore Greenland, Boessenkool et al. 2001). All scale bars = 10 µm.

Plate 6. 1–11. *Trinovantedinium variabile*. 1-6. Specimen from Saanich inlet (UVic 13-303-1, 48.59°N, 123.50°W, water depth 226 m). 7–9. Other specimen from sediment-trap from Saanich Inlet (UVic 09-183, slide 1, 48.65°N, 123.48°W, water depth 96 m), previously studied by Price and Pospelova (2011). 10–11. Scanning electron microscope photographs of two specimens from sample Exp37A from Saanich Inlet (48.55°N, 123.53W, water depth 215 m). Figures 12–14. *Selenopemphix undulata* from Brentwood Bay, BC, Canada, sequenced through single-cell PCR. All scale bars = 10 µm.

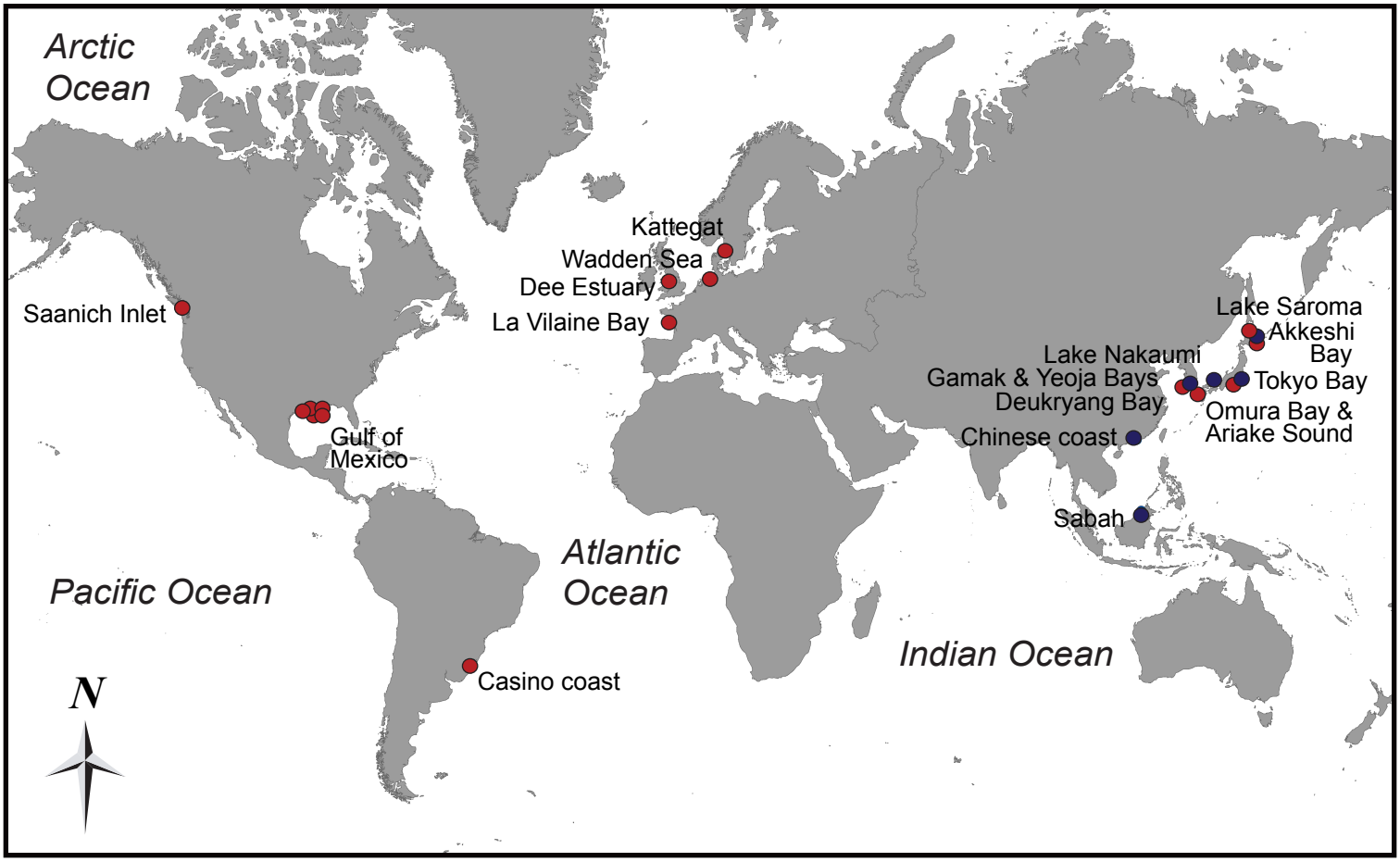
Arctic Ocean
Kattegat
Wadden Sea
Dee Estuary
La Vilaine Bay
Saanich Inlet
Lake Saroma
Akkeshi Bay
Lake Nakaumi
Gamak & Yeoja Bays
Tokyo Bay
Deukryang Bay
Omura Bay & Ariake Sound
Chinese coast
Gulf of Mexico
Sabah
Atlantic Ocean
Pacific Ocean
Indian Ocean
Casino coast
N

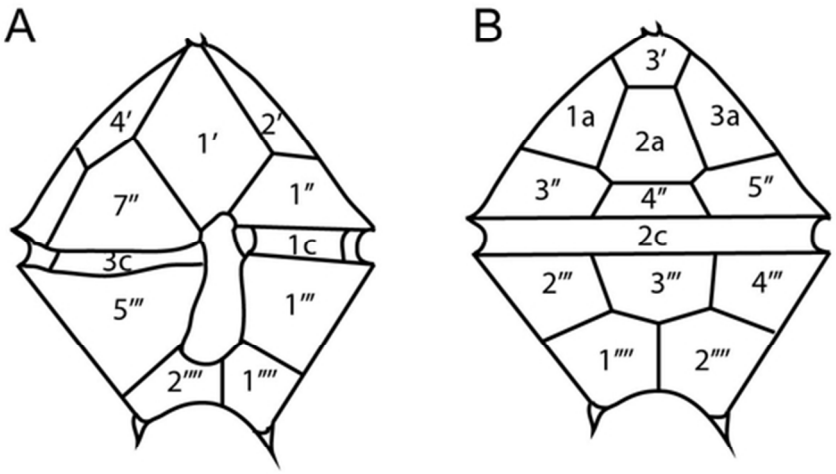

Figure 2. Drawings of Protoperidinium louisanensis n. sp. A). Ventral view. B). Dorsal view.
55x33mm (300 x 300 DPI)

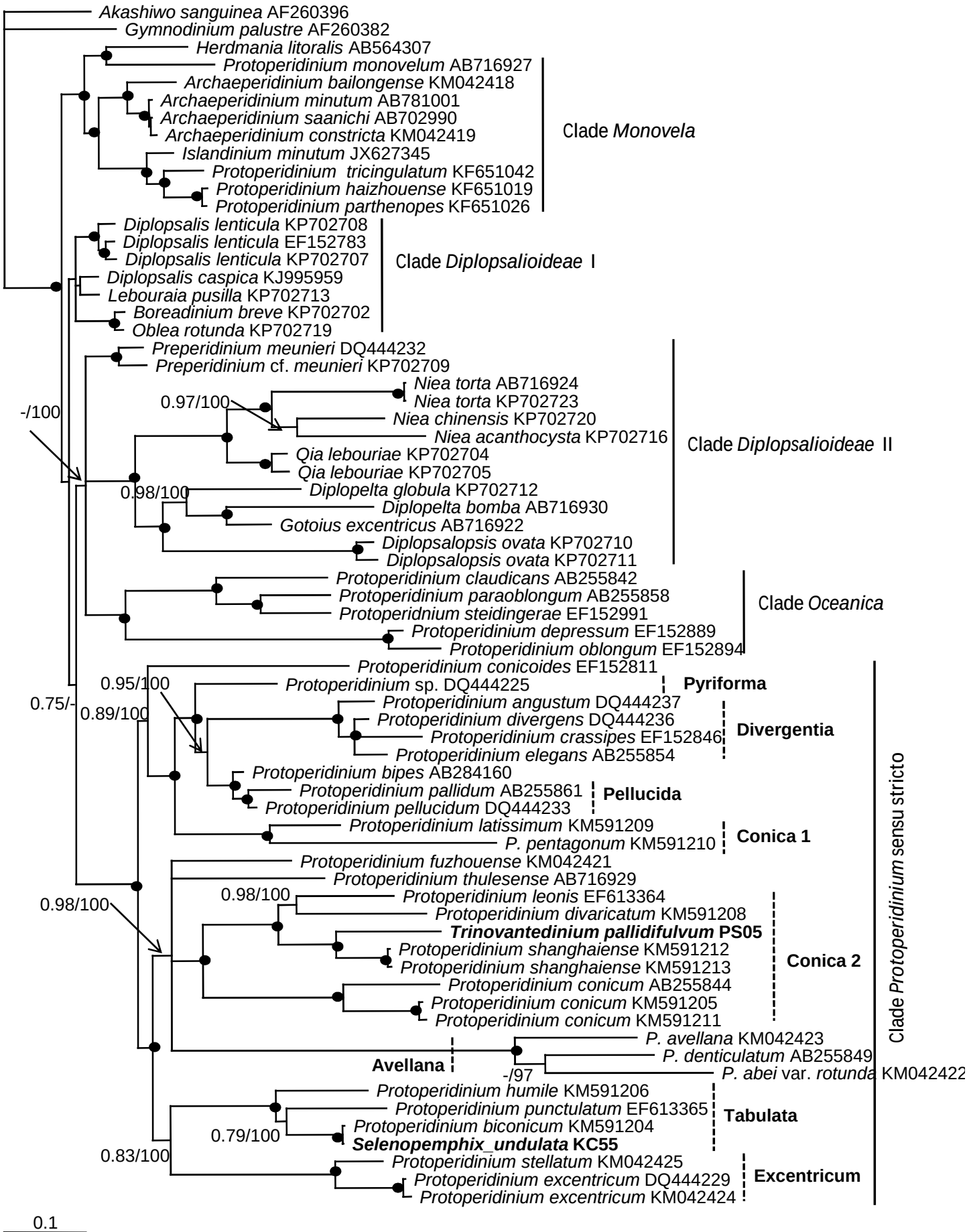
Akashiwo sanguinea AF260396
Gymnodinium palustre AF260382
Herdmania litoralis AB564307
Protoperidinium monovelum AB716927
Archaeperidinium bailongense KM042418
Archaeperidinium minutum AB781001
Archaeperidinium saanichi AB702990
Archaeperidinium constricta KM042419
Islandinium minutum JX627345
Protoperidinium tricingulatum KF651042
Protoperidinium haizhouense KF651019
Protoperidinium parthenopes KF651026
Clade Monovela
Diplopsalis lenticula KP702708
Diplopsalis lenticula EF152783
Diplopsalis lenticula KP702707
Diplopsalis caspica KJ995959
Lebouraia pusilla KP702713
Boreadinium breve KP702702
Oblea rotunda KP702719
Clade Diplopsalioideae I
Preperidinium meunieri DQ444232
Preperidinium cf. meunieri KP702709
Niea torta AB716924
Niea torta KP702723
Niea chinensis KP702720
Niea acanthocysta KP702716
Qia lebouriae KP702704
Qia lebouriae KP702705
Diplopelta globula KP702712
Diplopelta bomba AB716930
Gotoius excentricus AB716922
Diplopsalopsis ovata KP702710
Diplopsalopsis ovata KP702711
Clade Diplopsalioideae II
Protoperidinium claudicans AB255842
Protoperidinium paraoblongum AB255858
Protoperidnium steidingerae EF152991
Protoperidinium depressum EF152889
Protoperidinium oblongum EF152894
Clade Oceanica
Protoperidinium conicoides EF152811
Protoperidinium sp. DQ444225
Pyriforma
Protoperidinium angustum DQ444237
Protoperidinium divergens DQ444236
Protoperidinium crassipes EF152846
Protoperidinium elegans AB255854
Divergentia
Protoperidinium bipes AB284160
Protoperidinium pallidum AB255861
Protoperidinium pellucidum DQ444233
Pellucida
Protoperidinium latissimum KM591209
P. pentagonum KM591210
Conica 1
Protoperidinium fuzhouense KM042421
Protoperidinium thulesense AB716929
Protoperidinium leonis EF613364
Protoperidinium divaricatum KM591208
Trinovantedinium pallidifulvum PS05
Protoperidinium shanghaiense KM591212
Protoperidinium shanghaiense KM591213
Protoperidinium conicum AB255844
Protoperidinium conicum KM591205
Protoperidinium conicum KM591211
Conica 2
P. avellana KM042423
P. denticulatum AB255849
P. abei var. rotunda KM042422
Avellana
Protoperidinium humile KM591206
Protoperidinium punctulatum EF613365
Protoperidinium biconicum KM591204
Selenopemphix_undulata KC55
Tabulata
Protoperidinium stellatum KM042425
Protoperidinium excentricum DQ444229
Protoperidinium excentricum KM042424
Excentricum
Clade Protoperidinium sensu stricto
-/100
0.97/100
0.98/100
0.75/-
0.89/100
0.95/100
0.98/100
0.79/100
0.83/100
-/97
0.1

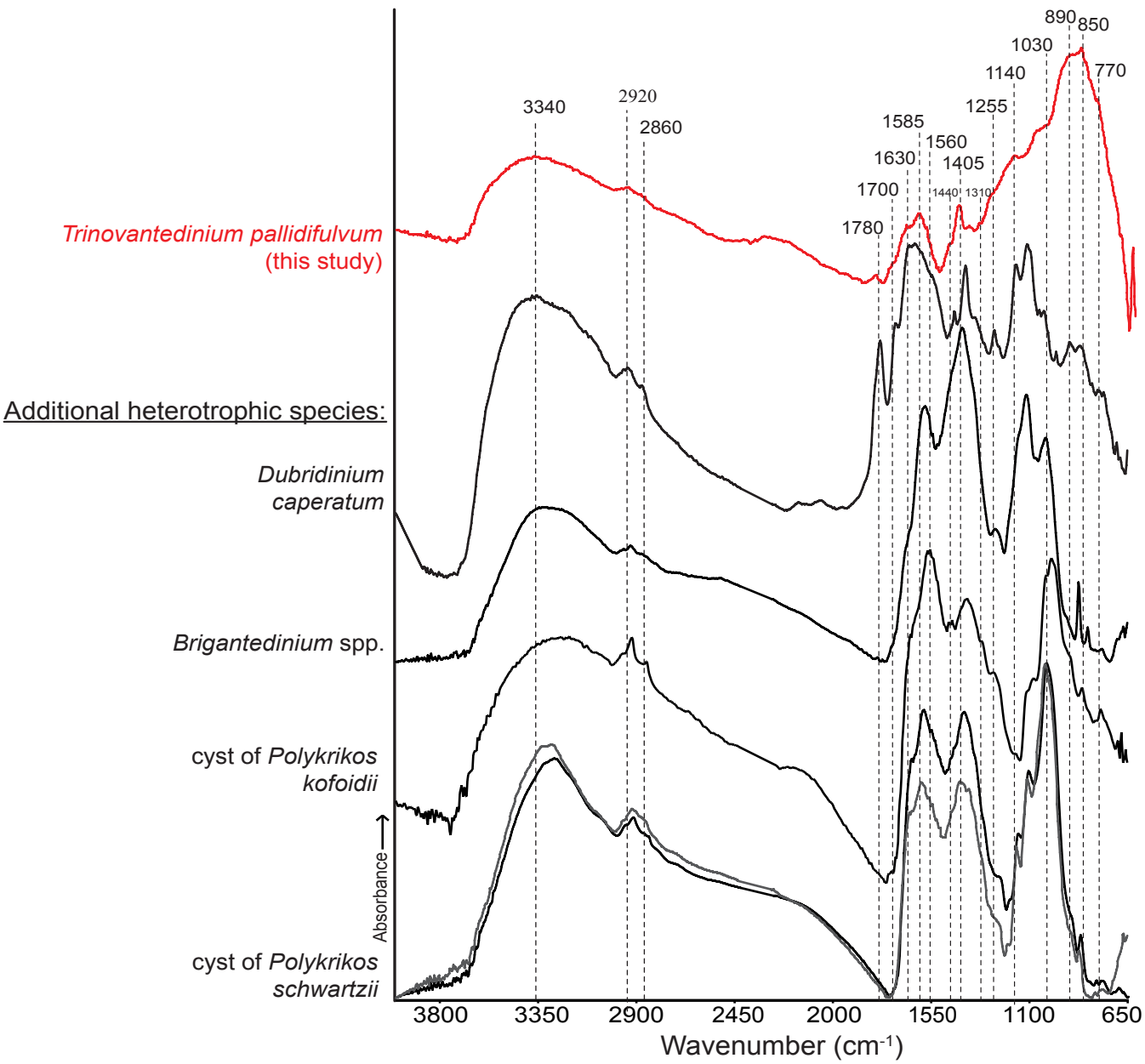
3340
2920
2860
1780
1700
1630
1585
1560
1440
1405
1310
1255
1140
1030
890
850
770
Trinovantedinium pallidifulvum (this study)
Additional heterotrophic species:
Dubridinium caperatum
Brigantedinium spp.
cyst of Polykrikos kofoidii
cyst of Polykrikos schwartzii
Absorbance
3800
3350
2900
2450
2000
1550
1100
650
Wavenumber (cm-1)

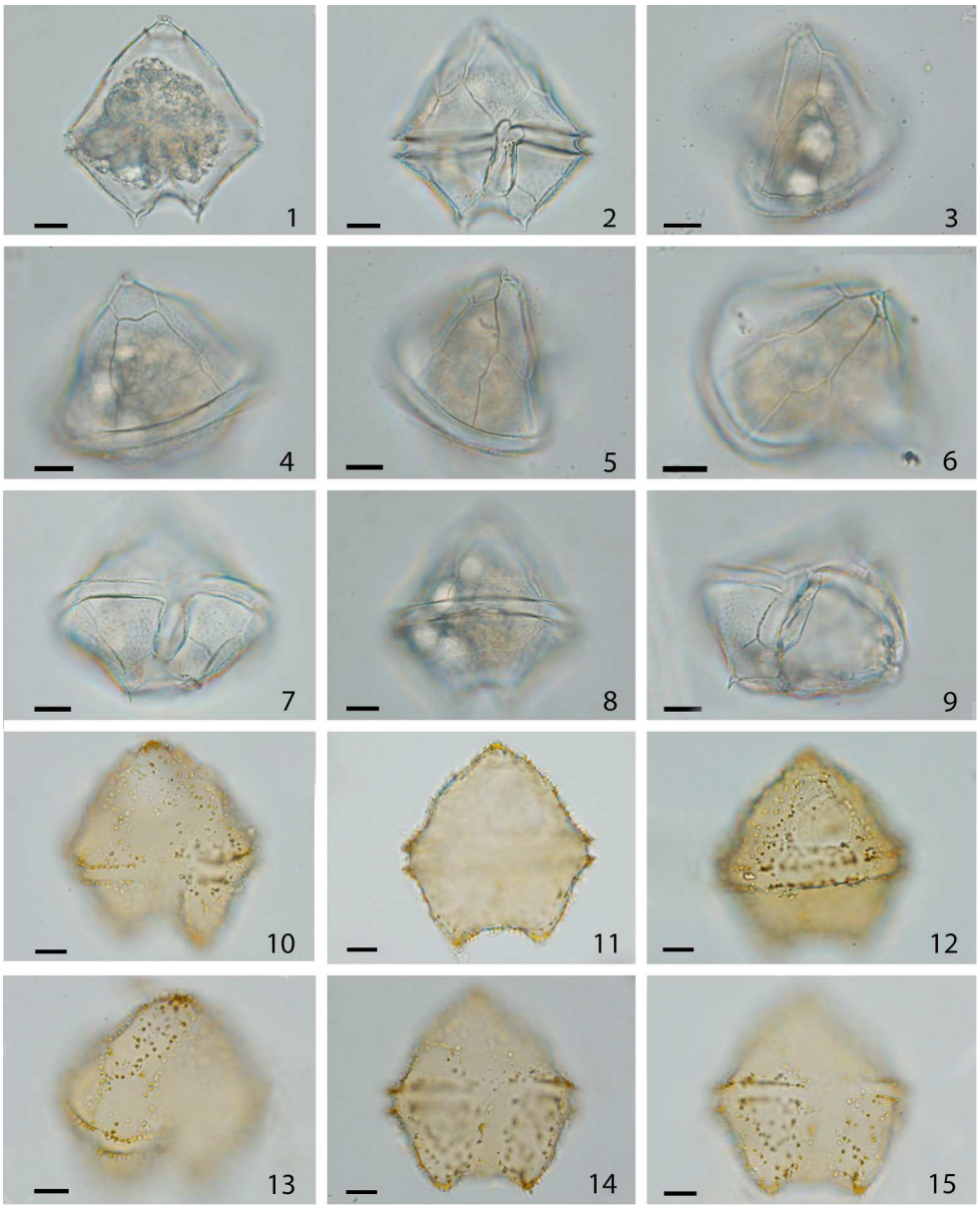

209x258mm (300 x 300 DPI)

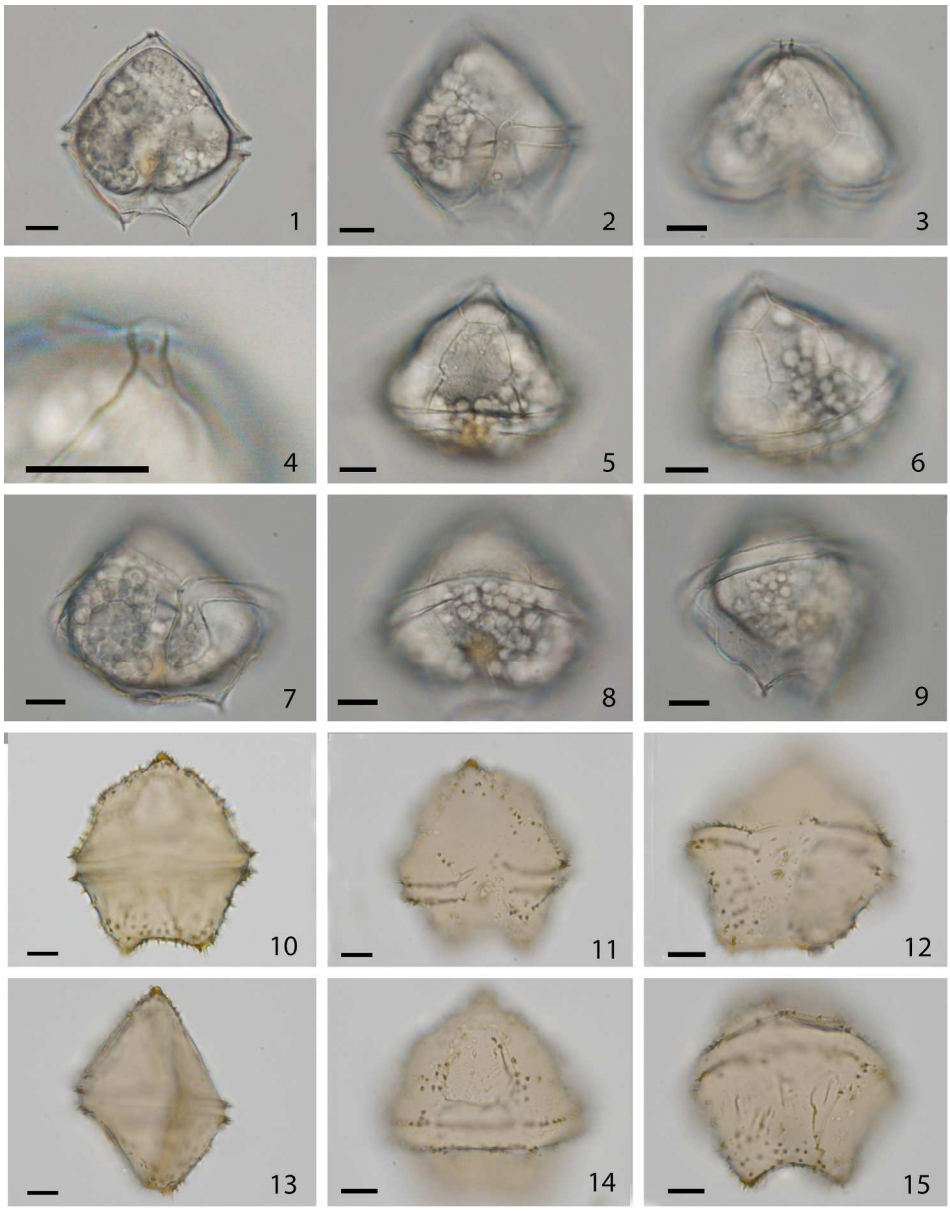

209x267mm (300 x 300 DPI)

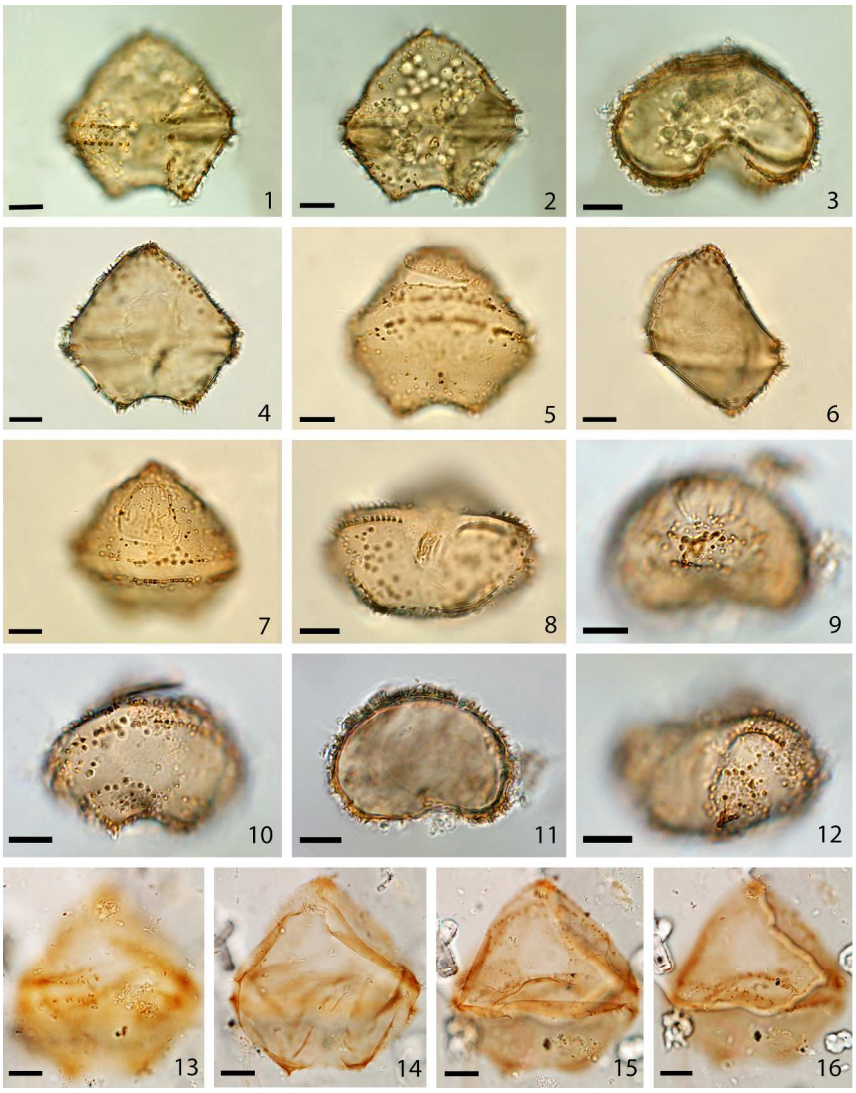

209x297mm (300 x 300 DPI)

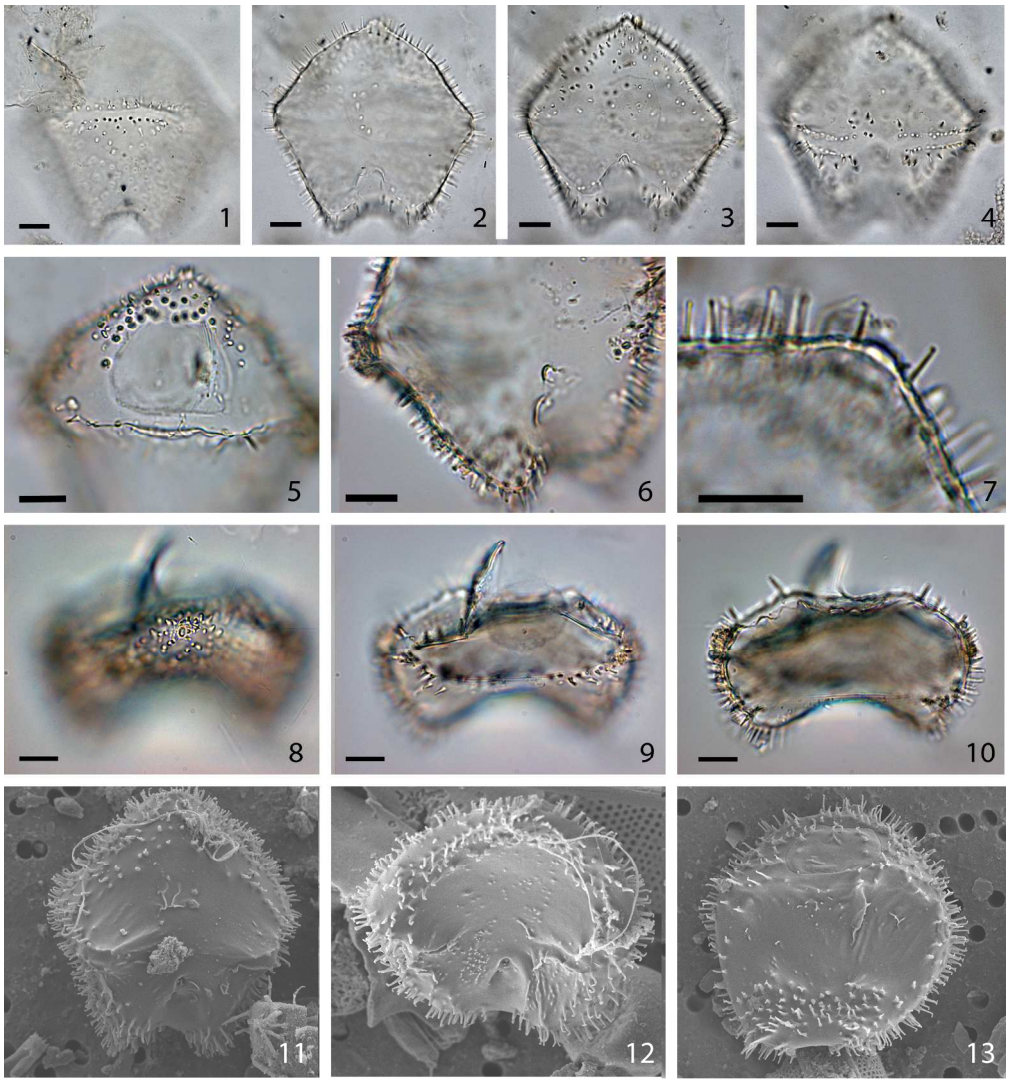

209x225mm (300 x 300 DPI)

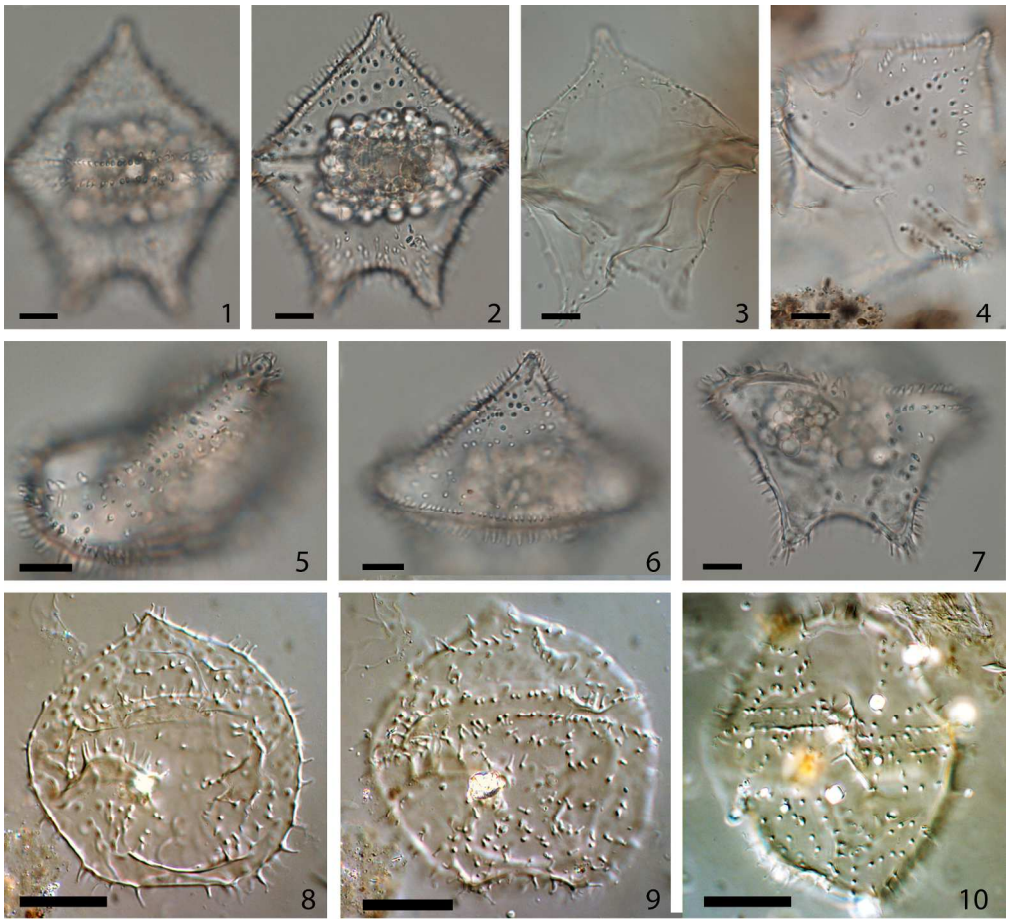

209x191mm (300 x 300 DPI)

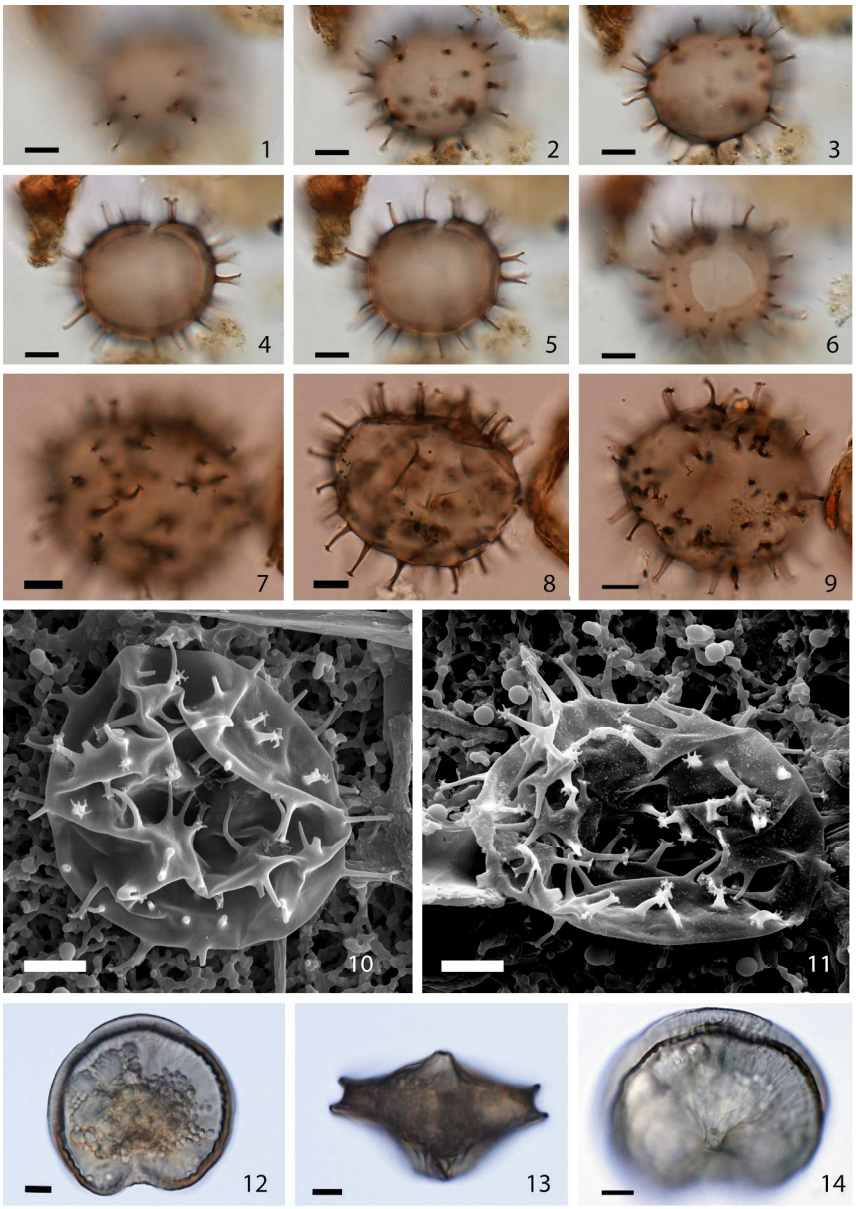

209x297mm (300 x 300 DPI)